Near-Wall Modelling of Compressible Turbulent Flows

by

Ronald M.C. So
Mechanical and Aerospace Engineering
Arizona State University
Tempe, AZ 85287

A Semi-Annual Progress Report Submitted

to

Dr. T. B. Gatski
NASA Langley Research Center
Hampton, VA 23665

under

Grant No. NAG-1-1080

December 31, 1990

Summary

This progress report summarizes the work carried out during the period July 1 to December 31, 1990. During this period, work has been carried out to formulate near-wall models for the equations governing the transport of the temperature-variance and its dissipation rate. With these equations properly modelled, a foundation is laid for their extension together with the heat-flux equations to compressible flows. This extension is carried out in a manner similar to that used to extend the incompressible near-wall Reynolds-stress models to compressible flows. In this report, the methodology used to accomplish the extension of the near-wall Reynolds-stress models is examined and the actual extension of the models for the Reynolds-stress equations and the near-wall dissipation-rate equation to compressible flows is given. Then the formulation of the near-wall models for the equations governing the transport of the temperature variance and its dissipation rate is discussed. Finally, a sample calculation of a flat plate compressible turbulent boundary-layer flow with adiabatic wall boundary condition and a free-stream Mach number of 2.5 using a two-equation near-wall closure is presented. The results show that the near-wall two-equation closure formulated for compressible flows is quite valid and the calculated properties are in good agreement with measurements. Furthermore, the near-wall behavior of the turbulence statistics and structure parameters is consistent with that found in incompressible flows.

Contents

Summary i

Contents ii

1. Program Objectives 1

2. Progress to date 2

3. Near-Wall Compressible Flow Models 4

3.1 Mean Flow Equations 4

3.2 Modelling of the Reynolds-Stress Equations 6

3.3 Modelling of the Dissipation-Rate Equation 12

3.4 Modelling of the Temperature Variance and its Dissipation Rate Equations 14

4. Compressible Boundary Layer on an Adiabatic Plate 23

4.1 Governing Equations and Turbulence Closure 23

4.2 Results and Discussion 25

4.3 Conclusions 28

5. Plans for Next Period 30

References 31

Figures 33

1. Program Objectives

With the availability of near-wall Reynolds-stress [1] and heat-flux models [2], the time is now ripe for their extension to flows where temperature cannot be considered as a passive scalar, such as in a compressible flow. This means that the transport equations for the temperature variance and its dissipation rate have to be solved simultaneously with the governing mean flow and energy equations, the Reynolds-stress equations and the heat-flux equations in a second-moment closure of the problem. Therefore, near-wall models for the equations governing the transport of the temperature variance and its dissipation rate are also required, in addition to the near-wall model for Reynolds stresses and heat fluxes. The present project attempts to accomplish these objectives using the approach outlined by Lai and So [1,2] in their modelling of incompressible near-wall Reynolds stresses and heat fluxes. More specifically, the present objectives can be stated as follows.

(1) To extend the near-wall Reynolds-stress and heat-flux models of Lai and So [1,2] to compressible flows and to modify the dissipation-rate equation so that it gives a correct near-wall behavior for the dissipation rate.

(2) To formulate a near-wall closure for the temperature-variance transport equation.

(3) To formulate a near-wall closure for the equation that governs the transport of the dissipation rate of the temperature variance.

(4) To extend all the above models to compressible flows.

(5) To validate these models using incompressible flow data, heat and mass transfer data and compressible flow data.

2. Progress to date

In the past year, work has been carried out to accomplish the first four objectives listed above. The extensions of the near-wall Reynolds-stress and heat-flux models to compressible flows have been effected by formulating the compressible flow equations into a form similar to their incompressible counterparts. Furthermore, the compressible dissipation function is split into a solenoidal part that is not influenced by compressibility effects and a dilatational part that is totally dependent on the turbulent Mach number. With this split, all closure models could be expressed in terms of the solenoidal dissipation rate. Therefore the incompressible limit of the compressible models could be recovered in a straight forward manner. An existing high-Reynolds-number dissipation-rate equation has been extended to describe the transport of the solenoidal dissipation rate and the resultant equation has been modified to give the correct near-wall behavior. This work has been reported previously by So et al. [3]. The same methodology is then used to treat the incompressible equations that govern the transport of the dissipation rate of the turbulent kinetic energy and the temperature variance and its dissipation rate. These studies have been completed and a brief discussion is given below in Section 3.

In addition, a validation of a near-wall, two-equation closure for compressible flows has been attempted. A compressible boundary layer with a free-stream Mach number of 2.5 on an adiabatic flat plate is considered. The near-wall, two-equation closure for compressible flows tested consists of solving the mean compressible flow equations plus the compressible form of the modelled turbulent kinetic energy and dilatational dissipation-rate equations. A turbulent Prandtl number is assumed for this initial validation of the two-equation closure. Once the two-equation closure has been validated, the turbulent-Prandtl-number assumption can be relaxed and the equations that govern the transport of the temperature variance and its dissipation rate will be solved to give the compressible turbulent heat flux. This way, the validity of the turbulent-Prandtl-number assumption could be assessed together with the models for the heat fluxes. The calculated

mean velocity and temperature profiles, wall shear and wall heat flux are in good agreement with measurements. Furthermore, the turbulence statistics and their associated structure parameters near the wall are consistent with those obtained in incompressible flows. This study has been completed and the results are presented in Section 4.

3. Near-Wall Compressible Flow Models

3.1 Mean Flow Equations

The compressible turbulent flow equations are obtained by applying Favre averaging to the instantaneous Navier-Stokes equations which for Newtonian fluids can be written as:

$$\frac{\partial \rho}{\partial t} + \frac{\partial}{\partial x_i}(\rho u_i) = 0 \quad , \tag{1}$$

$$\frac{\partial(\rho u_i)}{\partial t} + \frac{\partial}{\partial x_j}(\rho u_i u_j) = -\frac{\partial p}{\partial x_i} + \frac{\partial \tau_{ij}}{\partial x_j} \quad , \tag{2}$$

$$\frac{\partial(\rho C_p T)}{\partial t} + \frac{\partial}{\partial x_i}(\rho C_p T u_i) = \frac{\partial p}{\partial t} + u_i \frac{\partial p}{\partial x_i} + \frac{\partial}{\partial x}\left(\kappa \frac{\partial T}{\partial x_i}\right) + \tau_{ij}\frac{\partial u_i}{\partial x_j} \quad , \tag{3}$$

$$\text{where } \tau_{ij} = \mu\left(\frac{\partial u_i}{\partial x_j} + \frac{\partial u_j}{\partial x_i}\right) - \frac{2}{3}\mu \frac{\partial u_k}{\partial x_k}\delta_{ij} \quad , \tag{4}$$

u_i is the i^{th} component of the velocity vector, x_i is the i^{th} component of the coordinates and p, T, ρ, μ, κ, C_p are pressure, temperature and fluid properties, density, viscosity, thermal conductivity and specific heat at constant pressure, respectively. Favre decomposition is applied to all variables except p and ρ where conventional Reynolds decomposition is assumed. In other words

$$u_i = \langle U_i \rangle + u_i'' \quad , \tag{5a}$$

$$T = \langle \Theta \rangle + \theta'' \quad , \tag{5b}$$

$$p = \overline{P} + p' \quad , \tag{5c}$$

$$\rho = \overline{\rho} + \rho' \quad , \tag{5d}$$

where u_i'' and θ'' are the Favre fluctuations and p' and ρ' are the Reynolds fluctuations. If $< >$ is used to denote Favre-averaged quantities and the overbar the Reynolds-averaged quantities, then the turbulent equations become

$$\frac{\partial \overline{\rho}}{\partial t} + \frac{\partial}{\partial x_i}\left(\overline{\rho}\langle U_i\rangle\right) = 0 \ , \tag{6}$$

$$\frac{\partial}{\partial t}\left(\overline{\rho}\langle U_i\rangle\right) + \frac{\partial}{\partial x_j}\left(\overline{\rho}\langle U_i\rangle\langle U_j\rangle + \overline{\rho}\langle u_i'' u_j''\rangle\right) = -\frac{\partial \overline{P}}{\partial x_i} + \frac{\partial \langle \tau_{ij}\rangle}{\partial x_j} + \frac{\partial \overline{\tau_{ij}''}}{\partial x_j} \ , \tag{7}$$

$$\frac{\partial}{\partial t}\left(\overline{\rho}\,\overline{C_p}\langle\Theta\rangle\right) + \frac{\partial}{\partial x_i}\left(\overline{\rho}\,\overline{C_p}\langle\Theta\rangle\langle U_i\rangle + \overline{\rho}\,\overline{C_p}\,\langle\theta'' u_i''\rangle\right) = \frac{\partial}{\partial x_i}\left(\overline{\kappa}\frac{\partial\langle\Theta\rangle}{\partial x_i}\right) + \frac{\partial}{\partial x_i}\left(\overline{\kappa}\frac{\partial\overline{\theta''}}{\partial x_i}\right) + \frac{\partial \overline{P}}{\partial t}$$

$$+ \langle U_i\rangle\frac{\partial \overline{P}}{\partial x_i} + \overline{u_i''}\frac{\partial \overline{P}}{\partial x_i} \ \overline{u_i''\frac{\partial p'}{\partial x_i}} + \langle\tau_{ij}\rangle\frac{\partial\langle U_i\rangle}{\partial x_j} + \langle\tau_{ij}\rangle\frac{\partial\overline{u_i''}}{\partial x_j} + \overline{\tau_{ij}''}\frac{\partial\langle U_i\rangle}{\partial x_j} + \overline{\tau_{ij}''\frac{\partial u_i''}{\partial x_j}} \ , \tag{8}$$

where $\mu = \overline{\mu}$, $\kappa = \overline{\kappa}$ and $C_p = \overline{C_p}$ have been assumed and

$$\langle\tau_{ij}\rangle = \overline{\mu}\left(\frac{\partial\langle U_i\rangle}{\partial x_j} + \frac{\partial\langle U_j\rangle}{\partial x_i}\right) - \frac{2}{3}\overline{\mu}\,\delta_{ij}\frac{\partial\langle U_k\rangle}{\partial x_k} \ ,$$

$$\overline{\tau_{ij}''} = \overline{\mu}\left(\frac{\partial\overline{u_i''}}{\partial x_j} + \frac{\partial\overline{u_j''}}{\partial x_i}\right) - \frac{2}{3}\overline{\mu}\,\delta_{ij}\frac{\partial\overline{u_k''}}{\partial x_k} \ ,$$

represent the mean and time-averaged fluctuating stress tensor, respectively. These equations can be further simplified by assuming the turbulent flow to be stationary and by making use of the mean momentum equation (7), the Reynolds-stress and turbulent kinetic energy, $k = \frac{1}{2}\langle u_i'' u_i''\rangle$, equations to be derived later. The result is

$$\frac{\partial}{\partial x_i}\left(\overline{\rho}\langle U_i\rangle\right) = 0 \ , \tag{9}$$

$$\frac{\partial}{\partial x_j}\left(\overline{\rho}\langle U_i\rangle\langle U_j\rangle\right) = -\frac{\partial \overline{P}}{\partial x_i} + \frac{\partial \langle\tau_{ij}\rangle}{\partial x_j} - \frac{\partial}{\partial x_j}\left(\overline{\rho}\langle u_i''\rangle\langle u_j''\rangle\right) + \underline{\frac{\partial \overline{\tau_{ij}''}}{\partial x_j}} \quad , \tag{10}$$

$$\frac{\partial}{\partial x_i}\left(\overline{\rho}\langle U_i\rangle\left[\overline{C}_p\langle\Theta\rangle + \frac{1}{2}\langle U_k\rangle\langle U_k\rangle + k\right]\right) = \frac{\partial}{\partial x_i}\left(\overline{\kappa}\frac{\partial\langle\Theta\rangle}{\partial x_i}\right)$$

$$+ \frac{\partial}{\partial x_j}\left(\langle\tau_{ij}\rangle\langle U_i\rangle\right) - \frac{\partial}{\partial x_i}\left(\overline{\rho}\,\overline{C}_p\langle\theta'' u_i''\rangle\right) - \frac{\partial}{\partial x_i}\left(\overline{\rho}\langle u_i'' u_j''\rangle\langle U_j\rangle\right)$$

$$+ \underline{\frac{\partial}{\partial x_i}\left(\overline{\tau_{ij}''}\langle U_j\rangle\right)} - \underline{\frac{\partial}{\partial x_i}\left(\overline{\rho}\langle k\, u_i''\rangle\right)} + \underline{\frac{\partial}{\partial x_i}\left(\overline{u_j''\tau_{ij}''}\right)} + \underline{\frac{\partial}{\partial x_i}\left(\overline{u_j''}\langle\tau_{ij}\rangle\right)} + \underline{\frac{\partial}{\partial x_i}\left(\overline{\kappa}\frac{\partial\overline{\theta''}}{\partial x_i}\right)} \quad . \tag{11}$$

As a first approximation, the underlined terms could be neglected compared to the terms retained in (9) - (11). Thus formulated, the compressible flow equations are identical to the incompressible flow equations. In the latter case, $\overline{\rho}$ is constant and all the variables represent Reynolds-averaged quantities.

In the following, the modelling of the equations that govern the transport of $\overline{\rho}\langle u_i'' u_j''\rangle$ is first presented. This is followed by the modelling of the equations that govern the transport of the dissipation rate of the turbulent kinetic energy and the temperature variance and its dissipation rate.

3.2 Modelling of the Reynolds-Stress Equations

The Favre-averaged transport equation for the Reynolds stresses $\overline{\rho}\langle u_i'' u_j''\rangle$ could be similarly derived as in the incompressible case [1]. That is, the ith fluctuating equation is obtained by subtracting the mean momentum equation from the instantaneous equation. Repeat the same procedure to obtain the jth fluctuating equation. The ith fluctuating equation is then multiplied by the jth fluctuation velocity and vice versa. The two equations are then added together and averaged over time. Omitting all the algebra, the final exact equation is:

$$\frac{\partial}{\partial t}\left[\bar{\rho}\langle u_i'' u_j''\rangle\right] + \frac{\partial}{\partial x_k}\left[\bar{\rho}\langle U_k\rangle\langle u_i'' u_j''\rangle\right] = -\frac{\partial}{\partial x_k}\left[\bar{\rho}\langle u_i'' u_j'' u_k''\rangle\right] + \frac{\partial}{\partial x_k}\left[\overline{u_i'' \tau_{jk}''} + \overline{u_j'' \tau_{ik}''}\right]$$

$$-\left[\overline{\tau_{ik}'' \frac{\partial u_j''}{\partial x_k}} + \overline{\tau_{jk}'' \frac{\partial u_i''}{\partial x_k}}\right] - \left[\overline{u_i'' \frac{\partial p'}{\partial x_j}} + \overline{u_j'' \frac{\partial p'}{\partial x_j}}\right] - \left[\bar{\rho}\langle u_i'' u_k''\rangle \frac{\partial\langle U_j\rangle}{\partial x_k} + \bar{\rho}\langle u_j'' u_k''\rangle \frac{\partial\langle U_i\rangle}{\partial x_k}\right]$$

$$-\left[\overline{u_i''} \frac{\partial \bar{P}}{\partial x_j} + \overline{u_j''} \frac{\partial \bar{P}}{\partial x_i}\right] + \left[\overline{u_i''} \frac{\partial\langle\tau_{jk}\rangle}{\partial x_k} + \overline{u_j''} \frac{\partial\langle\tau_{ik}\rangle}{\partial x_k}\right] \quad . \tag{12}$$

Symbolically, the above equation can be written as

$$C_{ij} = D_{ij}^T + D^{*\nu}_{ij} - \bar{\rho}\varepsilon^*_{ij} + \Phi_{ij} + P_{ij} + G_{ij} + T_{ij} \quad . \tag{13}$$

With the exception of G_{ij} and T_{ij}, (13) is basically the same as its incompressible counterpart [1]. For an incompressible flow, $\overline{u_i''} \equiv 0$, and $G_{ij} = T_{ij} = 0$. Even under this condition, (13) fails to reduce properly to the incompressible equation given by Lai and So [1]. The reason is in the grouping of the terms $\left(D^{*\nu}_{ij} - \bar{\rho}\varepsilon^*_{ij} + \Phi_{ij}\right)$. In order to achieve this incompressible limit, a re-grouping of the terms in $\left(D^{*\nu}_{ij} - \bar{\rho}\varepsilon^*_{ij} + \Phi_{ij}\right)$ is necessary. If the viscous diffusion and dissipation terms in compressible flows are again defined similarly to their incompressible counterparts, or

$$D^{\nu}_{ij} = \frac{\partial}{\partial x_k}\left(\bar{\mu}\frac{\partial \overline{u_i'' u_j''}}{\partial x_k}\right) \quad , \tag{14}$$

$$\varepsilon_{ij} = 2\bar{\nu}\overline{\frac{\partial u_i'' \partial u_j''}{\partial x_k \partial x_k}} \quad , \tag{15}$$

then the terms $\left(D^{*\nu}_{ij} - \bar{\rho}\varepsilon^*_{ij} + \Phi_{ij}\right)$ can be re-grouped to give

$$D^{\nu}_{ij} - \bar{\rho}\varepsilon^*_{ij} + \Phi_{ij} = D^{\nu}_{ij} - \bar{\rho}\varepsilon_{ij} - \bar{\rho}\varepsilon^c_{ij} + \Phi^*_{ij} \tag{16}$$

where $\varepsilon^c_{ij} = \frac{\bar{\nu}}{3}\left(\overline{\frac{\partial u_i''}{\partial x_j}\frac{\partial u_k''}{\partial x_k}} + \overline{\frac{\partial u_j''}{\partial x_i}\frac{\partial u_k''}{\partial x_k}}\right)$, (17a)

$$\Phi_{ij}^{*} = -\left[\overline{u_i''\frac{\partial p'}{\partial x_j}} + \overline{u_j''\frac{\partial p'}{\partial x_i}}\right] + \frac{\bar{\mu}}{3}\left[\frac{\partial}{\partial x_j}\left(\overline{u_i''\frac{\partial u_k''}{\partial x_k}}\right) + \frac{\partial}{\partial x_i}\left(\overline{u_j''\frac{\partial u_k''}{\partial x_k}}\right)\right]$$

$$+ \frac{\partial \bar{\mu}}{\partial x_k}\left(\overline{u_i''\frac{\partial u_k''}{\partial x_j}} + \overline{u_j''\frac{\partial u_k''}{\partial x_i}}\right) - \frac{2}{3}\left[\frac{\partial \bar{\mu}}{\partial x_j}\overline{u_i''\frac{\partial u_k''}{\partial x_k}} + \frac{\partial \bar{\mu}}{\partial x_i}\overline{u_j''\frac{\partial u_k''}{\partial x_k}}\right]. \qquad (17b)$$

Note that (16) reduces to its incompressible counterpart exactly because $\partial \overline{u_i''}/\partial x_k \equiv 0$ and $\partial \bar{\mu}/\partial x_k \equiv 0$. For compressible flows, an extra term $\bar{\rho}\,\varepsilon_{ij}^{c}$ appears in (16). In addition, three additional terms are found in Φ_{ij}^{*}. The term $\bar{\rho}\,\varepsilon_{ij}^{c}$ is a dilatational term and could be interpreted as compressible or dilatational dissipation. This term is only important for compressible flows.

It should be pointed out that Φ_{ij}^{*} is given by (17b) and, as a result of this particular partitioning, there are several extra terms resulted from compressibility and variable viscosity. However, at high Reynolds number, dimensional arguments reveal that these extra contributions are not important. If pressure diffusion is further neglected, then the D_{ij}^{T}, $\bar{\rho}\,\varepsilon_{ij}$ and Φ_{ij}^{*} terms would assume the same form as their incompressible counterparts. Therefore, the high-Reynolds-number incompressible modelling of these terms could be naturally extended to the present case. However, a model for the compressible dissipation term $\bar{\rho}\,\varepsilon_{ij}^{c}$ is required in order to complete the closure. For high-Reynolds-number flows, this compressible dissipation could be assumed to be isotropic. As a result, the following model is proposed:

$$\varepsilon_{ij}^{c} = \frac{2}{3}\delta_{ij}\,\varepsilon^{c}$$

$$\text{where} \quad \varepsilon^{c} = \frac{\bar{\nu}}{3}\overline{\left(\frac{\partial u_k''}{\partial x_k}\right)^2} \quad . \qquad (18)$$

The modelling of ε^{c} has been attempted by Sarkar et al. [4]. They are the first to realize that the contribution of the dilatational dissipation term is important for supersonic and hypersonic flows. A simple algebraic model, which is based on an asymptotic analysis and a direct numerical

simulation of the simplified governing equations, has been proposed for ε^c. Their proposal could be modified for the present closure as

$$\varepsilon^c = 0.25\, M_t^2 \varepsilon \quad , \tag{19}$$

where $M_t^2 = 2k/\overline{c}^2$, $\overline{\rho}\varepsilon = \overline{\mu}\overline{\left(\frac{\partial u_i''}{\partial x_k}\right)^2}$ is the dissipation of k and $\overline{c}$ is the local mean speed of sound. Therefore, M_t is the local turbulent Mach number. It should be pointed out that Sarkar et al.'s definition of ε^c is four times larger than the present definition due to a different splitting of the terms in (16).

Once the high-Reynolds-number closure is obtained, the next important issue is to construct an asymptotically correct near-wall closure. To do so, near-wall behavior has to be analysed for each term in (13). This analysis is similar to the incompressible case except one more fluctuation ρ' has to be expanded and substituted into the exact equation. The expansions are:

$$\begin{aligned} u'' &= a_1 y + a_2 y^2 + \ldots \\ v'' &= b_1 y + b_2 y^2 + \ldots \\ w'' &= c_1 y + c_2 y^2 + \ldots \\ \rho' &= e_1 y + e_2 y^2 + \ldots \end{aligned} \tag{20}$$

It should be pointed out that, although the velocity expansions are physically correct, the expansion for density is an assumption. In general, the density fluctuation is not necessarily zero at the wall. Since ρ' is assumed to be essentially zero over the whole field in Morkovin's hypothesis, the present approach could be viewed as a partial relaxation of that assumption.

For incompressible flows, $b_1 = 0$ is obtained by imposing the incompressibility condition and becomes a crucial condition in near-wall analysis. This important condition holds the key to the present extension of the near-wall incompressible models to compressible flows. In order to show that b_1 indeed vanishes under these conditions, the continuity equation for density fluctuation ρ' is first derived, or

$$\frac{\partial \rho'}{\partial t} + \frac{\partial}{\partial x_k}\left(\overline{\rho} u_k'' + \rho' \langle U_k \rangle + \rho' u_k''\right) = 0. \tag{21}$$

Expansions (20) are then substituted into the above equation. If $\langle U_k \rangle = 0$ at the wall is used, it can be easily verified that $b_1 = 0$ is still a valid condition for compressible flows, irrespective of the thermal boundary condition. Therefore, the assumed ρ' expansion facilitates the modelling of compressible flows because all the expansions for compressible flows have similar forms as their incompressible counterparts except the extra ε_{ij}^c term which needs to be analyzed. Using the definition for ε_{ij}^c, it is easily verified that ε_{ij}^c is of order y^2 for the 11, 22, 33 and 13 components, while it is of order y for the 12 and 23 components. The high-Reynolds-number model proposal (19) provides higher order behavior when a wall is approached. Therefore, it is proposed that model (19) could be extended to near-wall flow without modification, while the near-wall balance provided by the exact ε_{ij}^c is taken into consideration by combining it with the Φ_{ij}^* term.

On the other hand, the same near-wall behavior as its incompressible counterpart is deduced for ε_{ij} and the incompressible model [2] could be extended to compressible flows. In other words, ε_{ij} could be modelled by

$$\varepsilon_{ij} = \frac{2}{3}(1 - f_{w,1})\varepsilon\delta_{ij} + f_{w,1}\frac{\varepsilon}{k}(\langle u_i'' u_j'' \rangle + \langle u_i'' u_k'' \rangle n_k n_j + \langle u_j'' u_k'' \rangle n_k n_i + \langle u_k'' u_m'' \rangle n_m n_k n_i n_j)$$

$$/\,(1 + 3\langle u_m'' u_k'' \rangle n_m n_k / 2k) \tag{22}$$

Near-wall analysis again shows that turbulent diffusion is a higher order term near a wall and its high-Reynolds-number model could be used because it does not affect the near-wall balance. Hanjalic and Launder's [5] model is suggested for this term. For compressible flows, their model could be modified to give

$$D_{ij}^T = \frac{\partial}{\partial x_k}\left(C_\varepsilon \frac{1}{\overline{\rho}} \frac{k}{\varepsilon}\left(\overline{\rho}\langle u_i'' u_m'' \rangle \frac{\partial \overline{\rho}\langle u_j'' u_k'' \rangle}{\partial x_m} + \overline{\rho}\langle u_j'' u_m'' \rangle \frac{\partial \overline{\rho}\langle u_k'' u_i'' \rangle}{\partial x_m} + \overline{\rho}\langle u_k'' u_m'' \rangle \frac{\partial \overline{\rho}\langle u_i'' u_j'' \rangle}{\partial x_m}\right)\right) . \tag{23}$$

The near-wall behavior of Φ_{ij}^{*} and $\overline{\rho}\varepsilon_{ij}^{c}$ together could be evaluated by using the exact equation (13). One difference from incompressible flows is the appearance of G_{ij} and T_{ij} in (13). Therefore, the near-wall behavior of G_{ij} and T_{ij} has to be analysed first before discussing the models for the combined term ($\Phi_{ij}^{*} + \overline{\rho}\varepsilon_{ij}^{c}$). The appearance of mean pressure in the G_{ij} term makes the analysis difficult. To circumvent this difficulty, the mean momentum equation (10) is substituted and the final analysis shows that the combined ($G_{ij} + T_{ij}$) term has the following near-wall behavior; namely,

$$G_{11} + T_{11} \rightarrow O(y^2)\ ;\ G_{33} + T_{33} \rightarrow O(y^2)\ ;\ G_{13} + T_{13} \rightarrow O(y^2)\ ,$$

$$G_{12} + T_{12} \rightarrow O(y^2)\ ;\ G_{23} + T_{23} \rightarrow O(y^2)\ ;\ G_{22} + T_{22} \rightarrow O(y^3)\ . \tag{24}$$

This means that, to the lowest order, the near-wall behavior of $\Phi_{ij}^{*} + \overline{\rho}\varepsilon_{ij}^{c}$ is similar to the incompressible case [2]. Therefore, the incompressible model could be extended to compressible flows as follows:

$$\varepsilon_{ij}^{c} = \frac{1}{6}M_t^2\varepsilon\delta_{ij}\ , \tag{25}$$

$$\Phi_{ij}^{*} + \overline{\rho}\varepsilon_{ij}^{c} = \Phi_{ij} + f_{w,1}\,\Phi_{ij,w}\ , \tag{26}$$

$$\Phi_{ij} = -C_1\,\overline{\rho}\,\frac{\varepsilon}{k}\left(\langle u_i'' u_j''\rangle - \frac{2}{3}\delta_{ij}k\right) - \alpha\left(P_{ij} - \frac{2}{3}\delta_{ij}\hat{P}\right)$$

$$- \beta\left(D_{ij} - \frac{2}{3}\delta_{ij}\hat{P}\right) - \gamma\,\overline{\rho}\,k\left(\frac{\partial\langle U_i\rangle}{\partial x_j} + \frac{\partial\langle U_j\rangle}{\partial x_i}\right)\ , \tag{27}$$

$$\Phi_{ij,w} = -C_1\,\overline{\rho}\,\frac{\varepsilon}{k}\left(\langle u_i'' u_j''\rangle - \frac{2}{3}\delta_{ij}k\right) - \overline{\rho}\,\frac{\varepsilon}{k}\left(\langle u_i'' u_k''\rangle n_k n_j + \langle u_j'' u_k''\rangle n_k n_i\right) + \alpha^{*}\left(P_{ij} - \frac{2}{3}\delta_{ij}\hat{P}\right), \tag{28}$$

with $$P_{ij} = -\,\overline{\rho}\left(\langle u_i'' u_k''\rangle\frac{\partial\langle U_j\rangle}{\partial x_k} + \langle u_j'' u_k''\rangle\frac{\partial\langle U_i\rangle}{\partial x_k}\right)\ ,$$

$$D_{ij} = -\,\overline{\rho}\left(\langle u_i'' u_k''\rangle\frac{\partial\langle U_k\rangle}{\partial x_j} + \langle u_j'' u_k''\rangle\frac{\partial\langle U_k\rangle}{\partial x_i}\right)\ ,$$

and $\hat{P} = P_{ii}/2$. The re-grouping suggested in (14) to (17) is now obvious, because the incompressible models could be straight-forwardly extended to near-wall compressible flows.

The proposed model still fails to close the equation because of the presence of T_{ij} and G_{ij} which are mutiplied by the term $\overline{u_k''}$. Therefore, it is necessary to shed some light on the modeling of $\overline{u_k''}$, which is equal to zero for an incompressible flow. Using Favre averaging, it can be shown that $-\overline{\rho' u_k''} = \bar{\rho}\overline{u_k''}$. In other words, $\overline{u_k''} = -\overline{\rho' u_k''}/\bar{\rho}$. Previous proposals for $-\overline{\rho' u_k''}$ are based on the gradient transport assumption; namely,

$$-\overline{\rho' u_k''} = \frac{\nu_t}{\sigma_\rho}\frac{\partial \bar{\rho}}{\partial x_k}, \tag{29}$$

where $\nu_t = C_\mu \frac{k^2}{\varepsilon}$. However, a more elaborate and probably 'better' way to model the term is to adopt the proposal,

$$\overline{u_k''} = -\frac{\overline{\rho' u_k''}}{\bar{\rho}} = C_\rho \frac{k}{\rho\varepsilon}\langle u_k'' u_j''\rangle \frac{\partial \bar{\rho}}{\partial x_j}. \tag{30}$$

Since these proposals are not consistent with the assumption of non-gradient transport, it is suggested that the following form is used to evaluate $\overline{u_k''}$ instead, or

$$\overline{u_k''} = \beta \frac{\overline{u_k'' \theta''}}{\langle\Theta\rangle}, \quad \text{with } \beta = -\left(\frac{\partial \bar{\rho}}{\partial\langle\Theta\rangle}\right)_p \frac{\langle\Theta\rangle}{\bar{\rho}}, \tag{31}$$

where β equals to unity for ideal gas.

3.3 Modeling of the Dissipation-Rate Equation

The exact transport equation for the dissipation rate of turbulent kinetic energy can be similarly derived as in the incompressible case. Omitting all the algebra, the exact compressible equation for ε is given by

$$\frac{D\bar{\rho}\varepsilon}{Dt} = 2\bar{\nu}\frac{\partial}{\partial x_k}\left[\overline{\frac{\partial u_i''}{\partial x_j}\frac{\partial \tau_{ik}''}{\partial x_j}}\right] - \frac{\partial}{\partial x_k}\left[\bar{\rho}\langle u_k\,\varepsilon\rangle + 2\bar{\nu}\overline{\frac{\partial p'}{\partial x_i}\frac{\partial u_k''}{\partial x_i}}\right]$$

$$- 2\bar{\rho}\bar{\nu}\frac{\partial \langle U_i\rangle}{\partial x_k}\left[\langle\frac{\partial u_i''}{\partial x_j}\frac{\partial u_k''}{\partial x_j}\rangle + \langle\frac{\partial u_j''}{\partial x_i}\frac{\partial u_j''}{\partial x_k}\rangle\right]$$

$$- 2\bar{\rho}\bar{\nu}\,\langle u_k''\frac{\partial u_i''}{\partial x_j}\rangle\frac{\partial^2\langle U_i\rangle}{\partial x_k\partial x_j} - 2\bar{\rho}\bar{\nu}\langle\frac{\partial u_i''}{\partial x_k}\frac{\partial u_i''}{\partial x_j}\frac{\partial u_k''}{\partial x_j}\rangle$$

$$- 2\bar{\nu}\overline{\frac{\partial^2 u_i''}{\partial x_k\partial x_j\partial x_k}\frac{\partial \tau_{ij}''}{\partial x_k}} + 2\bar{\rho}\bar{\nu}\overline{\frac{\partial u_i''}{\partial x_k}\frac{\partial f_{ij}'}{\partial x_k}} + S_{\varepsilon 1} + S_{\varepsilon 2}\quad . \tag{32}$$

It has been pointed out that the ε-equation is the most difficult to model even for incompressible flows [3]. Obviously, due to a lack of measurements in compressible flows, a rigorous modelling of the compressible ε-equation is not possible at the present time. The best suggestion probably is to extend the incompressible model to compressible flows. There are two important extra terms resulted from compressibility effects which will otherwise disappear. These terms are:

$$S_{\varepsilon 1} = -2\bar{\nu}\overline{\frac{\partial u_i''}{\partial x_k}\frac{\partial^2 \bar{P}}{\partial x_k\partial x_i}} \quad \text{and} \quad S_{\varepsilon 2} = 2\bar{\nu}\overline{\frac{\partial u_i''}{\partial x_k}\frac{\partial^2\langle\tau_{ij}\rangle}{\partial x_k\partial x_j}}\quad . \tag{33}$$

Along the suggestion of Jones [6] for high-Reynolds-number flows, the above terms could be modelled as

$$S_{\varepsilon 1} = -C_{\varepsilon 3}\frac{\varepsilon}{k}\overline{u_k''}\frac{\partial \bar{P}}{\partial x_k} \quad \text{and} \quad S_{\varepsilon 2} = C_{\varepsilon 4}\bar{\rho}\varepsilon\frac{\partial\langle U_k\rangle}{\partial x_k}\quad . \tag{34}$$

For near-wall flows, these models require modifications because it is obvious that $S_{\varepsilon 1}$ becomes infinite when a wall is approached. A simple way is to replace ε by $\tilde{\varepsilon} = \varepsilon - \varepsilon_w$ in the above expressions where ε_w is the value of ε at the wall. In summary, the ε-equation for a compressible flow could be modelled as

$$\frac{\partial \bar{\rho}\varepsilon}{\partial t} + \frac{\partial \bar{\rho}\langle U_k\rangle \varepsilon}{\partial x_k} = \frac{\partial}{\partial x_k}\left(\bar{\mu}\frac{\partial \varepsilon}{\partial x_k}\right) + \frac{\partial}{\partial x_k}\left(C_\varepsilon \frac{\bar{\rho}k}{\varepsilon}\langle u_k'' u_i''\rangle \frac{\partial \varepsilon}{\partial x_i}\right) + C_{\varepsilon 1}\frac{\varepsilon}{k}\hat{P} - C_{\varepsilon 2} f_\varepsilon \bar{\rho}\frac{\tilde{\varepsilon}\tilde{\varepsilon}}{k}$$
$$- C_{\varepsilon 3}\frac{\tilde{\varepsilon}}{k}\overline{\rho u_k''}\frac{\partial \bar{P}}{\partial x_k} + C_{\varepsilon 4}\bar{\rho}\tilde{\varepsilon}\frac{\partial \langle U_k\rangle}{\partial x_k} + f_{w,2}\bar{\rho}\left(\left(\frac{7}{9}C_{\varepsilon 2} - 2\right)\frac{\tilde{\varepsilon}\tilde{\varepsilon}}{k} - \frac{1}{2}\frac{\overline{\varepsilon''^2}}{k}\right) \qquad (35)$$

The incompressible form of this equation is identical to that proposed by Lai and So [1]. Unfortunately, the incompressible equation fails to give the correct ε behavior near a wall. So et al. [3] have recently carried out a study to investigate the near-wall behavior of the incompressible transport equation for ε. They found that if the f_ε and $f_{w,2}$ terms in (35) are modified to give $\left(-C_{\varepsilon 2} f_2 \frac{\bar{\rho}\varepsilon^2}{k}\right)$, where f_2 is given by

$$f_2 = \frac{\tilde{\varepsilon}}{\varepsilon}\left[1 + \frac{2f_{w,2}}{C_{\varepsilon 2}} - \frac{3}{2}\frac{f_{w,2}}{C_{\varepsilon 2}}\frac{\varepsilon^{*2}}{\tilde{\varepsilon}\tilde{\varepsilon}}\right] , \qquad (36)$$

then the predicted ε behavior in the near-wall region is in good agreement with direct simulation data [7-9]. Here $\varepsilon^* = \varepsilon - 2\overline{\nu}k/y^2$. Consequently, the terms,

$$- C_{\varepsilon 2} f_\varepsilon \frac{\bar{\rho}\tilde{\varepsilon}\tilde{\varepsilon}}{k} + f_{w,2}\bar{\rho}\left[\left(\frac{7}{9}C_{\varepsilon 2} - 2\right)\frac{\tilde{\varepsilon}\tilde{\varepsilon}}{k} - \frac{1}{2}\frac{\overline{\varepsilon''^2}}{k}\right],$$

in (35) is replaced by $\left[-C_{\varepsilon 2} f_2 \frac{\bar{\rho}\varepsilon^2}{k}\right]$ and the resultant ε-equation is asymptotically correct as a wall is approached.

3.4 Modelling of the Temperature Variance and its Dissipation Rate Equations

In near-wall modelling of the compressible Reynolds-stress and dissipation-rate equations, effort is made to recast the equations to a form similar to their incompressible counterparts. This

means that all terms with explicit compressibility effects are grouped together so that when the incompressible limit is approached, they will go to zero identically and the other terms in the compressible equations will approach their corresponding terms in the incompressible equations. Thus formulated, the incompressible near-wall models could be extended to compressible flows in a straight forward manner. The only new models required are those for the terms with explicit compressibility effects. However, this approach, attractive though it seems, requires the knowledge of well tested incompressible near-wall models. For the Reynolds-stress and dissipation-rate equations, the incompressible near-wall models are provided by Lai and So [1]. As for the heat-flux and temperature variance and its dissipation-rate equations, a complete incompressible near-wall closure is not available. Lai and So [2] proposed a near-wall closure for the incompressible heat-flux equations. However, they did not propose near-wall models for the temperature variance and its dissipation rate equaations. In this section, an attempt is made to model these two equations in the near-wall region. An incompressible closure is first sought. After these equations have been properly modelled for near-wall flows, they and the near-wall heat-flux equations [2] will be used as a base for extension to compressible flows.

If the temperature variance is denoted by $\overline{\theta^2}$ and the dissipation rate of $\overline{\theta^2}$ is defined by

$$\varepsilon_\theta = \alpha \overline{\frac{\partial \theta}{\partial x_k}\frac{\partial \theta}{\partial x_k}} \quad , \tag{37}$$

where $\alpha = \kappa/\rho C_p$ is the thermal diffusivity, then the exact equations governing $\overline{\theta^2}$ and ε_θ are given by

$$\frac{\partial \overline{\theta^2}}{\partial t} + \frac{\partial}{\partial x_k}\left(U_k \overline{\theta^2}\right) = \frac{\partial}{\partial x_k}\left(\alpha \frac{\partial \overline{\theta^2}}{\partial x_k}\right) - \frac{\partial}{\partial x_k}\left(\overline{u_k' \theta^2}\right) - 2\overline{u_k' \theta}\frac{\partial \Theta}{\partial x_k} - 2\alpha \overline{\frac{\partial \theta}{\partial x_k}\frac{\partial \theta}{\partial x_k}} + 2\overline{\theta S_\theta} \quad , \tag{38}$$

$$\frac{\partial \varepsilon_\theta}{\partial t} + \frac{\partial}{\partial x_k}(U_k \varepsilon_\theta) = \frac{\partial}{\partial x_k}\left(\alpha \frac{\partial \varepsilon_\theta}{\partial x_k}\right) - \frac{\partial}{\partial x_k}\left(\overline{u_k' \varepsilon_\theta}\right) - 2\alpha \overline{\frac{\partial \theta}{\partial x_j}\frac{\partial u_k'}{\partial x_j}\frac{\partial \Theta}{\partial x_k}} - 2\alpha \overline{u_k' \frac{\partial \theta}{\partial x_j}\frac{\partial^2 \Theta}{\partial x_k \partial x_j}}$$

$$- 2\alpha \overline{\frac{\partial \theta}{\partial x_j}\frac{\partial \theta}{\partial x_k}\frac{\partial U_k}{\partial x_j}} - 2\alpha \overline{\frac{\partial \theta}{\partial x_j}\frac{\partial u_k'}{\partial x_j}\frac{\partial \theta}{\partial x_k}} - 2\overline{\left(\alpha \frac{\partial^2 \theta}{\partial x_k \partial x_j}\right)^2} + 2\alpha \overline{\frac{\partial \theta}{\partial x_j}\frac{\partial s_\theta}{\partial x_j}} \quad , \tag{39}$$

where U_i is the component of the Reynolds-averaged mean velocity, u_i'' its fluctuating velocity component, θ is the fluctuating temperature and s_θ is the source term involving the fluctuating viscous stress and fluctuating velocity gradient.

It is clear from the exact transport equations (38) and (39) that the relative importance of the different terms in the $\overline{\theta^2}$ and ε_θ budgets is similar to those of the corresponding terms in the turbulent kinetic energy and dissipation-rate equations. Several experimental studies have shown that the close similarity between k and ε and $\overline{\theta^2}$ and ε_θ budgets do exist. For example, the measurements by Krishnamoorthy and Antonia [10,11] for a turbulent boundary layer indicated that the thermal and velocity fields resemble each other. Particularly, the measurements of ε_θ have enabled the temperature dissipation time scale to be estimated in the near-wall region and approximately the same distribution as the velocity dissipation time scale was obtained.

Most proposals used to model the $\overline{\theta^2}$ equation have adopted a gradient-type representation for $\overline{u_k \theta^2}$. In order to be consistent with the velocity field, the following form could be suggested

$$- \overline{u_k \theta^2} = C_s^{\theta^2} \frac{\overline{u_k u_j}}{\varepsilon} \frac{k}{\varepsilon} \frac{\partial \overline{\theta^2}}{\partial x_j} \quad . \tag{40}$$

As far as the near-wall flow is concerned, asymptotic analysis shows that this turbulent diffusion is negligible compared with the dissipation and molecular diffusion terms in (38). Furthermore, experimental measurements [10,11] support this assumption. Consequently, (40) could be easily extended to near-wall flows. The diffusion coefficient $C_s^{\theta^2}$ could be chosen as 0.11 as recommended by Launder [12].

The more important term requiring approximation in the $\overline{\theta^2}$ equation is the dissipation rate ε_θ. In most previous studies, this dissipation rate is algebraically related to $\overline{\theta^2}$ through the use of a time-scale ratio R [12,13] and the time-scale ratio was chosen to be 0.5 to 0.8 depending on the flow cases considered. Unfortunately, measurements for the decay of temperature and velocity fluctuations behind a heated grid suggested that the time-scale ratio has a rather wide scatter and is not sufficiently constant to serve as a general method for the determination of ε_θ. The alternative then is to determine ε_θ from its own transport equation which is given in (39).

The problem of closing (39) is much more difficult than that of the ε-equation because there are more time and generation-rate scales in the ε_θ-equation. For high-Reynolds-number flows, dimensional analysis suggests that only the 6th and 7th terms on the RHS of (39) are important. These terms bear a close resemblance to the corresponding terms in the ε-equation. Several proposals have been made to close the ε_θ-equation for high-Reynolds-number flows [14-18]. Among them, the closure suggested by Jones and Musonge [14] takes the following form:

$$\frac{D\varepsilon_\theta}{Dt} = D^t_{\varepsilon\theta} + P_{\varepsilon\theta} - \Sigma_{\varepsilon\theta} \quad , \tag{41}$$

$$\text{with} \quad P_{\varepsilon\theta} = C_{d2}\frac{\varepsilon}{k}P_\theta + C_{d3}\,\varepsilon_\theta\frac{P}{k} \quad , \tag{42}$$

$$\Sigma_{\varepsilon\theta} = C_{d4}\frac{\varepsilon_\theta}{\overline{\theta^2}} + C_{d5}\frac{\varepsilon}{k}\varepsilon_\theta \quad , \tag{43}$$

$$\text{with} \quad P_\theta = -\overline{u_k\theta}\frac{\partial\Theta}{\partial x_k} \quad \text{and} \quad P = -\overline{u_iu_j}\frac{\partial U_i}{\partial x_j} \quad . \tag{44}$$

Note that in the modelling of the terms, $P_{\varepsilon\theta}$ and $\Sigma_{\varepsilon\theta}$, involving the generation and destruction of fine scale turbulence interactions, both the thermal and velocity time scales are used. In the second-order models of Newman et al. [15] and Eighobashi and Launder [16], however, only the thermal time scale and the thermal production rate are used for $P_{\varepsilon\theta}$, i.e.,

$$P_{\varepsilon\theta} = C_{d1} \frac{\varepsilon_\theta}{\theta^2} P_\theta \quad , \tag{45}$$

while in the model of Nagano and Kim [17],

$$P_{\varepsilon\theta} = C_{d1} \frac{\varepsilon_\theta}{\theta^2} P_\theta + C_{d3} \varepsilon_\theta \frac{P}{k} \quad , \tag{46}$$

is proposed. It is worth noting that recently Yoshizawa [18] is able to arrive at the same form as (43) and (46) for the ε_θ closure by using the statistical results from a two-scale direct-interaction approximation. Even the model constants predicted from their direct-interaction approximation are close to the ones used by Nagano and Kim [17], Newman et al. [15] and Elghobashi and Launder [16].

Although it is generally agreed that both the temperature and velocity time scales and production rates affect ε_θ, all the above models only take one of the time scales and production rates into consideration. Therefore, it would seem that a more general form for $P_{\varepsilon\theta}$ would be

$$P_{\varepsilon\theta} = C_{d1} \frac{\varepsilon_\theta}{\theta^2} P_\theta + C_{d2} \frac{\varepsilon}{k} P_\theta + C_{d3} \varepsilon_\theta \frac{P}{k} \tag{47}$$

where the values of the model constants C_{d1} to C_{d5} are to be discussed later.

Finally, to close the ε_θ-equation, the turbulence diffusion, i.e. the 2nd term on the RHS of equation (39), could be similarly modelled through gradient-type approximation as the ε-equation; namely,

$$D^t_{\varepsilon\theta} = \frac{\partial}{\partial x_k} \left(C_s^{\varepsilon\theta} \frac{k}{\varepsilon} \overline{u_k u_j} \frac{\partial \varepsilon_\theta}{\partial x_j} \right) \tag{48}$$

In summary, the high-Reynolds-number $\overline{\theta^2}$ and ε_θ equations could be modelled in the following form:

$$\frac{D\overline{\theta^2}}{Dt} = \frac{\partial}{\partial x_k}\left(C_s^{\theta^2}\,\overline{u_k u_j}\,\frac{k}{\varepsilon}\,\frac{\partial\overline{\theta^2}}{\partial x_j}\right) + 2\overline{u_k'\theta}\,\frac{\partial\Theta}{\partial x_k} - 2\varepsilon_\theta \quad , \tag{49}$$

$$\frac{D\varepsilon_\theta}{Dt} = \frac{\partial}{\partial x_k}\left(C_s^{\varepsilon\theta}\,\frac{k}{\varepsilon}\,\overline{u_k u_j}\,\frac{\partial\varepsilon_\theta}{\partial x_j}\right) + C_{d1}\,\frac{\varepsilon_\theta}{\overline{\theta^2}}\,P_\theta + C_{d2}\frac{\varepsilon}{k}P_\theta + C_{d3}\,\varepsilon_\theta\frac{P}{k} - C_{d4}\,\frac{\varepsilon_\theta}{\overline{\theta^2}}\,\varepsilon_\theta - C_{d5}\frac{\varepsilon}{k}\,\varepsilon_\theta \quad . \tag{50}$$

Since a near-wall closure is to be formulated, an extension of the above equations to near-wall flows is required. This could be achieved in a manner analogous to the modelling of the k and ε equations. First of all, the viscous diffusion terms should be included in the equations, that is,

$$D_{\overline{\theta^2}}^{\alpha} = \frac{\partial}{\partial x_k}\left(\alpha\,\frac{\partial\overline{\theta^2}}{\partial x_k}\right) \quad , \tag{51}$$

$$D_{\varepsilon\theta}^{\alpha} = \frac{\partial}{\partial x_k}\left(\alpha\,\frac{\partial\varepsilon_\theta}{\partial x_k}\right) \quad . \tag{52}$$

With the addition of the viscous diffusion term to (49), it can be shown that the modelled equation is in balance to the lowest order in the near-wall region. Essentially, the balance is provided by molecular diffusion and viscous dissipation. This can be verified by the use of the expansions (20) and (39) for the definition of ε_θ. In view of this, the $\overline{\theta^2}$ equation, just like its counterpart k equation, needs no further modifications for near-wall flows.

A similar near-wall asymptotic analysis of the ε_θ-equation shows that the molecular diffusion term reaches a finite value at the wall and is dominant in the near-wall region. Near-wall analysis of other terms in (39) reveals that the generation terms are of higher order in y, while the destruction terms approach infinite values as a wall is approached because ε and ε_θ are finite and k and $\overline{\theta^2}$ are zero at the wall. This difficulty could be removed by replacing ε and ε_θ by $\tilde{\varepsilon}$ and $\tilde{\varepsilon_\theta}$ in (43), or

$$\Sigma_{\varepsilon\theta} = C_{d4}\,\frac{\tilde{\varepsilon_\theta}}{\overline{\theta^2}}\,\varepsilon_\theta + C_{d5}\frac{\tilde{\varepsilon}}{k}\,\varepsilon_\theta \quad , \tag{53}$$

$$\text{with} \quad \tilde{\varepsilon}_\theta = \varepsilon_\theta - \alpha\left(\frac{\partial\sqrt{\overline{\theta^2}}}{\partial y}\right)^2 \quad \text{and} \quad \tilde{\varepsilon} = \varepsilon - 2\nu\left(\frac{\partial\sqrt{k}}{\partial y}\right)^2 \quad . \tag{54}$$

Thus modified, the near-wall behavior of the modelled ε_θ-equation has the property that molecular diffusion and destruction become dominant when a wall is approached. This behavior is consistent with experimental observations and is analogous to the behavior of the ε-equation.

Despite the above modifications, the molecular diffusion and destruction terms generally are not in balance near a wall. However, a near-wall analysis similar to the ε-equation could be carried out for the ε_θ-equation to ensure that certain near-wall constraints are met. This can be accomplished by expanding the fluctuating quantities according to (20). Using the definitions of $\overline{\theta^2}$ and ε_θ and the substitution of (20), the following is obtained,

$$\begin{aligned} \overline{\theta^2} &= 2A\ y^2 + 2B\ y^3 + C\ y^4 + \ldots \quad , \\ \varepsilon_\theta &= \alpha\ (2A\ + 4B\ y + D\ y^2 + \ldots) \quad , \end{aligned} \tag{55}$$

where A, B, C and D are related to the time average of the coefficients d_1, d_2,.... Further analysis of the $\overline{\theta^2}$ equation at a wall yields

$$\varepsilon_\theta = \frac{\alpha}{2}\frac{\partial^2\overline{\theta^2}}{\partial x_k \partial x_k} \quad . \tag{56}$$

Following the suggestion of Shima [19] for the ε-equation, a transport equation of the right hand side of (56) could be derived and its behavior analyzed at a wall. This results in

$$\frac{\partial}{\partial t}\left(\alpha\frac{\partial^2\overline{\theta^2}}{\partial x_k \partial x_k}\right) = -2\alpha\frac{\partial^2\varepsilon_\theta}{\partial x_k \partial x_k} + \alpha\frac{\partial^2}{\partial x_m \partial x_m}\left(\alpha\frac{\partial^2\overline{\theta^2}}{\partial x_k \partial x_k}\right) \quad . \tag{57}$$

These two equations indicate that $2\partial\varepsilon_\theta/\partial t$ and the right-hand side of (57) should possess the same near-wall asymptotic behavior. This constraint could be used to further modify the ε_θ equation for near-wall flows.

Since a general analysis is difficult, the following analysis is restricted to the case where the averaged quantities are only functions of y and t (distance normal to a wall and time). The near-wall asymptotic behavior of the right-hand-side of (57) could be easily obtained by the substitution of expansions (20) and (55) and the result is $(-4\alpha^2 D+24\alpha^2 C)$. If the $\partial\varepsilon_\theta/\partial t$ equation is considered, it could be shown that a closure is required such that the left-hand-side of (57) would give the same value at the wall. It is sufficient to point out that an extra term $\psi_{\varepsilon\theta}$ is required for the ε_θ equation in order to satisfy the above constraint and it could be deduced as

$$\psi_{\varepsilon\theta} = f_{w,\varepsilon_\theta}\left((C_{d4}-4)\frac{\tilde{\varepsilon}_\theta}{\overline{\theta^2}}\varepsilon_\theta + C_{d5}\frac{\varepsilon}{k}\varepsilon_\theta - \frac{\varepsilon_\theta^{*2}}{\overline{\theta^2}}\right) , \tag{58}$$

with $\varepsilon_\theta^* = \varepsilon_\theta - \frac{\alpha\overline{\theta^2}}{y^2}$.

To verify that (58) indeed satisfies the modelled $\partial\varepsilon_\theta/\partial t$ behavior of $(-2\alpha^2 D+12\alpha^2 C)$, the following near-wall expansions could be obtained by using (20) and (57):

$$\sqrt{\overline{\theta^2}} = \sqrt{2A}\,y + (B/\sqrt{2A})\,y^2 + 2(C/\sqrt{2A})\,y^3 - \left(4B^2/\sqrt{2A^3}\right)y^3 + O(y^4) , \tag{59}$$

$$\tilde{\varepsilon}_\theta = \alpha\left(D - \frac{B^2}{2A} - 3C\right)y^2 + O(y^3) , \tag{60}$$

$$\frac{\varepsilon_\theta\tilde{\varepsilon}_\theta}{\overline{\theta^2}} = \alpha^2\left(D - \frac{B^2}{2A} - 3C\right) + O(y) , \tag{61}$$

$$\frac{\varepsilon_\theta^{*2}}{\overline{\theta^2}} = 2\alpha^2\frac{B^2}{2A} + O(y) . \tag{62}$$

In summary, the final $\overline{\theta^2}$ and ε_θ equations could be modelled as:

$$\frac{D\overline{\theta^2}}{Dt} = \frac{\partial}{\partial x_k}\left(\alpha\frac{\partial\overline{\theta^2}}{\partial x_k}\right) + \frac{\partial}{\partial x_k}\left(C_s^{\theta^2}\,\overline{u_k u_j}\frac{k}{\varepsilon}\frac{\partial\overline{\theta^2}}{\partial x_j}\right) - 2\overline{u_k'\theta}\,\frac{\partial\Theta}{\partial x_k} - 2\varepsilon_\theta , \tag{63}$$

$$\frac{D\varepsilon_\theta}{Dt} = \frac{\partial}{\partial x_k}\left(\alpha \frac{\partial \varepsilon_\theta}{\partial x_k}\right) + \frac{\partial}{\partial x_k}\left(C_s^{\varepsilon\theta} \frac{k}{\varepsilon} \overline{u_k u_j} \frac{\partial \varepsilon_\theta}{\partial x_j}\right) + C_{d1} \frac{\varepsilon_\theta}{\theta^2} P_\theta$$

$$+ C_{d2} \frac{\varepsilon}{k} P_\theta + C_{d3}\, \varepsilon_\theta \frac{P}{k} - C_{d4} \frac{\tilde{\varepsilon}_\theta}{\theta^2} \varepsilon_\theta - C_{d5} \frac{\tilde{\varepsilon}}{k} \varepsilon_\theta + \psi_{\varepsilon\theta} \qquad (64)$$

By considering the data obtained in decaying homogeneous scalar turbulence and temperature variance measurements in grid turbulence, Jones and Musonge [14] was able to determine the following model constants: $C_{d2} = 1.7$, $C_{d3} = 1.4$, $C_{d4} = 2.0$, $C_{d5} = 0.52$ with the C_{d1} term set equal to zero. Yoshizawa [18], on the other hand, estimated these constants using direct interaction approximation. His results are: $C_{d1} = C_{d4} = 1.2$, $C_{d3} = C_{d5} = 0.52$ and $C_{d2} = 0.0$. Newman et al. [15] optimized the model constants to give $C_{d1} = 1.0$, $C_{d4} = 1.01$, $C_{d5} = 0.88$ while Elghobashi and Launder [16] proposed the following values, $C_{d1} = 0.9$, $C_{d4} = 1.1$, $C_{d5} = 0.80$ with the C_{d2} and C_{d3} terms excluded. Nagano and Kim [17], however, adopted the same values as Elghobashi and Launder [16] except that the C_{d3} term is included and $C_{d3} = 0.72$ is suggested. It can be seen that all proposed constants are approximately of the same order of magnitude and more experimental and numerical studies are required to determine their proper values.

4. Compressible Boundary Layer on an Adiabatic Plate

4.1 Governing Equations and Turbulence Closure

The compressible boundary layer on an adiabatic flat plate is considered. If the usual boundary-layer approximations are made to simplify the governing equations, then equations (9) - (11) can be written as

$$\frac{\partial}{\partial x}\left(\overline{\rho}\,\langle U\rangle\right)+\frac{\partial}{\partial y}\left(\overline{\rho}\,\langle V\rangle\right) = 0 \quad , \tag{65}$$

$$\overline{\rho}\,\langle U\rangle\frac{\partial\langle U\rangle}{\partial x}+\overline{\rho}\,\langle V\rangle\frac{\partial\langle U\rangle}{\partial y}=\frac{\partial}{y}\left[\left(\overline{\mu}+\overline{\mu}_t\right)\frac{\partial\langle U\rangle}{\partial y}\right] \quad , \tag{66}$$

$$\overline{\rho}\,\langle U\rangle\frac{\partial\langle H\rangle}{\partial x}+\overline{\rho}\,\langle V\rangle\frac{\partial\langle H\rangle}{\partial y}=\frac{\partial}{\partial y}\left[\left(\frac{\overline{\mu}}{\mathrm{Pr}}+\frac{\overline{\mu}_t}{\mathrm{Pr}_t}\right)\frac{\partial\langle H\rangle}{\partial y}+\overline{\mu}\left(1-\frac{1}{\mathrm{Pr}}+\frac{\overline{\mu}_t}{\overline{\mu}}\right)\langle U\rangle\frac{\partial\langle U\rangle}{\partial y}\right] \quad , \tag{67}$$

where the gradient-transport assumption has been used to relate the turbulent momentum and heat fluxes to the mean gradients of velocity and temperature, respectively. In the process, a turbulent viscosity is assumed for compressible flows. This is a first attempt to validate the k-ε closure deduced above for near-wall compressible flows, therefore, a constant turbulent Prandtl number is assumed so that the turbulent heat conductivity coefficient can be related to the turbulent viscosity. The k-ε closure used to closed the above set of equations is given by the contraction of the modelled form of (12) and (35). Their exact form will be given below. It should be pointed out in here that the energy equation (67) is written in terms of the total enthalpy $\langle H\rangle$, which is the sum of the enthalpy $\langle h\rangle$, the mean kinetic energy $(\langle U\rangle)^2/2$ and the turbulent kinetic energy k.

The turbulent viscosity μ_t is related to k and ε by $C_\mu f_\mu \overline{\rho} k^2/\varepsilon$, while k and ε are obtained by solving their respective transport equations. A modelled k-equation valid all the way to the wall can be deduced by contracting (12) after applying the models proposed in (22), (23), (25) and (26)

for ε_{ij}, D_{ij}^T, ε_{ij}^c and Φ_{ij}^*, respectively. On the other hand, the near-wall ε-equation is given by (35).

Again, the boundary-layer approximations are used to simplify these equations and the results are:

$$\bar{\rho}\langle U\rangle\frac{\partial k}{\partial x}+\bar{\rho}\langle V\rangle\frac{\partial k}{\partial y}=\frac{\partial}{\partial y}\left[\left(\bar{\mu}+\frac{\bar{\mu}_t}{\sigma_k}\right)\frac{\partial k}{\partial y}\right]+\bar{\mu}_t\left(\frac{\partial\langle U\rangle}{\partial y}\right)^2-\bar{\rho}(\varepsilon+\varepsilon^c)$$
$$-(\gamma+\frac{2}{3})\bar{\rho}k\left(\frac{\partial\langle U\rangle}{\partial x}+\frac{\partial\langle V\rangle}{\partial y}\right)+\overline{u''}\frac{\partial}{\partial y}\left(\bar{\mu}\frac{\partial\langle U\rangle}{\partial y}\right)\quad,\tag{68}$$

$$\bar{\rho}\langle U\rangle\frac{\partial \varepsilon}{\partial x}+\bar{\rho}\langle V\rangle\frac{\partial \varepsilon}{\partial y}=\frac{\partial}{\partial y}\left[\left(\bar{\mu}+\frac{\bar{\mu}_t}{\sigma_\varepsilon}\right)\frac{\partial \varepsilon}{\partial y}\right]+C_{\varepsilon 1}\frac{\varepsilon}{k}\overline{\mu_t}\left(\frac{\partial\langle U\rangle}{\partial y}\right)^2$$
$$-C_{\varepsilon 2}f_2\frac{\bar{\rho}\varepsilon^2}{k}+C_{\varepsilon 3}\frac{\varepsilon}{k}\overline{u''}\frac{\partial}{\partial y}\left(\bar{\mu}\frac{\partial\langle U\rangle}{\partial y}\right)\quad,\tag{69}$$

In (69), the near-wall correction of So et al.[3] has been substitued. The reason is the more correct predicted behavior of ε in the near-wall region. The definitions of $\tilde{\varepsilon}$, ε^* and f_μ are given by

$$\tilde{\varepsilon}=\varepsilon-2\bar{\nu}\left(\frac{\partial\sqrt{k}}{\partial y}\right)^2\quad,\tag{70}$$

$$\varepsilon^*=\varepsilon-2\bar{\nu}\frac{k}{y^2}\quad,\tag{71}$$

$$f_\mu=(1+3.45/\sqrt{R_t})\tanh(y^+/120)\quad,\tag{72}$$

where $R_t=k^2/\bar{\nu}\varepsilon$, $y^+=yu_\tau/\bar{\nu}$, $u_\tau=\sqrt{(\tau_w/\rho)}$ and $\overline{u''}$ is defined by

$$\overline{u''}=\frac{\bar{\mu}_t}{\sigma_\rho\bar{\rho}^2}\frac{\partial\bar{\rho}}{\partial x}\quad.\tag{73}$$

Finally, the model constants are chosen as: $C_\mu = 0.096$, $C_{\varepsilon 1} = 1.50$, $C_{\varepsilon 2} = 1.83$, $\sigma_k = 1.01$, $\sigma_\varepsilon = 1.45$, $\sigma_\rho = 4.0$ and $\gamma = 0.18182$, and the turbulent Prandtl number Pr_t is assumed to be 0.7. The molecular Prandtl number Pr for air is calculated assumming it to be temperature dependent and the Sutherland law is used to evaluate the fluid viscosity at the appropriate temperature.

The boundary conditions are no slip at the wall for the velocities and zero heat flux at the wall for the enthalpy. At the edge of the boundary layer, the free-stream conditions are assumed for both the stream velocity and the enthalpy. Thus formulated, the above equations and the appropriate boundary conditions can be solved numerically using the boundary-layer code developed by So et al.[3].

4.2 Results and Discussion

The closure is used to calculate a flat plate supersonic boundary-layer flow [20], where the thermal wall boundary condition is adiabatic and the free stream Mach number is 3.701. This case is also calculated using a near-wall two-equation closure proposed in Ref. 21. Furthermore, some mean flow data of this case can be found in Ref. 22. Since it is a flat plate boundary-layer flow, there is no streamwise pressure gradient. For comparison purposes, the C_f data is taken from Ref. 20 while the other data is obtained from Ref. 22, where $C_f = 2\tau_w/(\rho_w U_e^2)$ is the skin friction coefficient. Here, the subscripts w and e are used to denote wall and free stream condition, respectively. In this case, the reported C_f at $Re_x = 1.939 \times 10^7$ is 1.246×10^{-3}. The two-equation model calculations of Ref. 21 are also compared with the present results whenever possible. This way, the strength and weaknesses of the near-wall closure could be assessed carefully.

The present objectives are to validate the two-equation near-wall closure and to analyse the calculated near-wall asymptotic behavior. Near the wall, the flow is essentially dominated by viscosity and the Mach number is very low irrespective of the free stream Mach number. Consequently, the near-wall asymptotic behavior of a flat plate compressible boundary layer should be quite similar to its incompressible counterpart. One of the present objective is to determine the extent of validity of this similarity, if indeed such a similarity exists. In other words, the wall behavior of k^+/y^{+2} = constant, $k^+/y^{+2}\varepsilon^+ = 0.5$, $-\overline{uv}^+/y^{+3}$ = constant and $-\overline{v\theta}^+/y^{+3}$ = constant should also be valid for flat plate compressible boundary layers. Here, the wall friction velocity is used to normalize k, ε and $-\overline{uv}$ while the free stream quantities are used to normalize $-\overline{v\theta}$

to give the dimensionless quantities. The extent of the similarity could then be determined from the y^+ value where these relations cease to be valid.

The present calculations are carried out with a thermal energy equation that is identical to that used in Ref. 21. This means that the term, $\partial[\overline{\mu_t}\langle U\rangle\partial\langle U\rangle/\partial y]/\partial y$, in (67) is neglected. Furthermore, k is omitted in the definition of $\langle H\rangle$. The influence of these terms on the calculated results is being investigated at present. However, their overall effects could not be large because these terms are one order of magnitude smaller than the terms retained in the final equation. The rationale for using the same thermal energy equation as Ref. 21 is to better assess the effects of the additional compressible terms in the k and ε equations.

The calculated C_f at the same x location is $1.253\text{x}10^{-3}$. This represents an error of <0.6% compared to the reported value [20,22]. The mean flow results are plotted in Figs. 1-3. In these figures, the measurements and the calculations using the model of Ref. 21 are also shown for comparison. There are several ways to define y^+ for compressible flows. Here, it is defined with the fluid propreties evaluated at the wall. The mean velocity (U^+) plot is shown versus $\ln y^+$ (Fig. 1), while the mean temperature ($\langle\Theta\rangle/\langle\Theta\rangle_e$) and total enthalpy ($\langle H\rangle/\langle H\rangle_e$) plots are shown versus y^+ (Figs. 2 and 3). It can be seen that the present results are in good agreement with data and with the calculations obtained from the model of Ref. 21. There is a slight discrepancy in the mean temperature and total enthalpy profiles near the wall. The present results give a fuller profile for both propreties. On the other hand, the model of Ref. 21 give a slight overshoot for the total enthalpy profile inside the boundary layer. This, of course, is not reasonable and could be the reason for the under-prediction of $\langle H\rangle$ near the wall. One of the reason could be the less correct near-wall turbulence model [21] compared to the present closure. More will be said about this point when the near-wall propreties are examined.

The near-wall distributions of the turbulent quantities are plotted in Figs. 4-7. In these plot, y^+ is defined using local fluid propreties. Since there are no measurements in this region, the

comparisons are made with the calculations obtained using the model of Ref. 21 whenever possible. It can be seen that the present prediction of ε^+ in the near-wall region is totally different from the model of Ref. 21. The present calculation is similar to that obtained by Spalart [9] through direct simulation of the Navier-Stokes equations. It is essentially identical to the distribution obtained by So et al. [3] for the case of an incompressible boundary layer. On the other hand, the calculation of ε^+ is about the same for both models for $y^+ > 35$. This means that the near-wall closure of Ref. 21 is not quite correct and could contribute to an incorrect prediction of H in the near-wall region. Further evidence that the near-wall model of Ref. 21 is not quite correct could be gleaned from the near-wall plots of k^+, $-\overline{uv}^+$ and $-\overline{v\theta}^+$ (Figs. 5-7). The model of Ref. 21 gives a k^+ distribution that is quite a bit lower than the present calculation. For example, the peak value of k^+ is calculated to be about 3.1 using the model of Ref. 21 (Fig. 5), while the present calculation gives a value of about 5.2. This latter value is in agreement with that obtained by Spalart [9] and So et al. [3] for an incompressible boundary layer. Furthermore, the drop of k^+ after the maximum is relatively steep for the present closure, while it is essentially constant for the model of Ref. 21. This behavior is also incorrect compared to incompressible flow data. The low value of k^+ suggests that turbulence is being severely damped in the near-wall region and this, in turn, could influence momentum and heat transport and could possibly lead to lower values for $-\overline{uv}^+$ and $-\overline{v\theta}^+$. The overall distributions of k^+, $-\overline{uv}^+$ and $-\overline{v\theta}^+$ are shown in Figs. 8-10, respectively. It can be seen that the model [21] prediction of k^+ in the outer region agrees well with the present result.

Finally, the near-wall asymptotic behavior of the turbulent propreties are examined in Figs. 11-14. The slope of k^+ versus y^{+2} is indeed constant and is equal to 0.094 (Fig. 11); a value that is about 4% lower than that obtained by So et al [3]. Therefore, it follows that the wall value of ε^+ is 0.188 and again is in very good agreement with the incompressible value [3]. On the other hand, the ratio $k^+/y^{+2}\varepsilon^+$ is 0.501 (Fig. 12) and verifies that expansions (20) are valid for compressible flows. This implies that there is great similarity between incompressible and

are also constant and are very small (Figs. 13 and 14). These results are consistent with incompressible flow calculations. However, the region in which the slopes are constant is limited to $y^+ = 1.0$. This compares with a region of $y^+ = 2.0$ for incompressible flows. Therefore, compressibility tends to decrease the region in which expansions (20) is valid, but it fails to eliminate this region altogether. Perhaps, when the free stream Mach number is sufficiently high, this viscosity dominated near-wall region will become so thin that it could be considered to be essentially non-existent.

It should be pointed out that the above results are obtained with a $C_{\varepsilon 2}f_2 = 1.83f_2(1.0 + \beta M_\infty^2)$ where β is determined to be 0.0044 based on a series of calculations at different M_∞. One could interpret this to mean that $C_{\varepsilon 2}$ is Mach number dependent, or it could be assumed that f_2 is influenced by M_∞. Based on the physics of near-wall flows, it would seem reasonable to assume f_2 to be dependent on M_∞. This assumption would keep intact the closure's ability to predict decaying turbulence in a homogeneous field. Another point to note are the additional compressible terms in (68) and (69). If these additional terms are neglected, the calculated near-wall behavior is very much like that given by Ref. 21. In other words, these terms are very important and are probably solely responsible for the correct prediction of compressible turbulence in the near-wall region. This means that compressiblility effects on the turbulence field could not be correctly modelled by a simple extension of the incompressible equations to compressible flows. The additional terms in the turbulence equations are partly responsible for the compressibility effects. Therefore, these terms should be retained in the modelled equations if the compressibility effects were to be accounted for properly.

4.3 Conclusions

The present calculations and comparisons help bring out the following points. These are:

(i) Morkovin's postulate [23] is justified as far as the calculation of the mean field is concerned. On the other hand, the calculation of the turbulence field is not quite correct if compressibility

effects were assumed to be solely accounted for by the variable mean density. This is particularly true in the near-wall region where Morkovin's postulate would lead to a drastic under-prediction of the turbulence propreties.

(ii) The additional compressible terms in the k and ϵ equations play a significant role in the calculation of near-wall turbulence. If these terms are neglected, compressibility effects on turbulence could not be accounted for properly and the result is under-prediction of the turbulence propreties.

(iii) These additional terms are responsible for providing the correct near-wall asymptotic behavior for the turbulence propreties. With their inclusion, the near-wall asymptotic behavior of compressible flows is found to be similar to that of incompressible flows. This result is reasonable because viscosity dominates in the very near-wall region.

(iv) The expansions (20) are found to be valid for the present calculations. Their validity for other thermal boundary condition remains to be verified.

5. Plans for Next Period

The plans for the next period are:

(i) To further validate the compressible near-wall k-ε closure, such as applying it to calculate other types of boundary-layer flows.

(ii) To validate the compressible near-wall Reynolds-stress closure by applying it to calculate the boundary-layer flow on an adiabatic plate and compare the results with measurements and the calculations of the compressible near-wall k-ε closure. In both calculations, a constant turbulent Prandtl number is assumed. This assumption will be relaxed after the near-wall compressible heat-flux models are formulated and their incompressible counterparts are properly validated.

(iii) To validate the incompressible near-wall $\overline{\theta^2}$-ε_θ closure using plane channel flow data with heat transfer. The data sets are chosen from direct simulation calculations as well as from measurements. They will cover both types of boundary conditions; that of constant wall heat flux and constant wall temperature.

References

1. Lai, Y.G. and So, R.M.C., "On near-wall turbulent flow modelling," *Journal of Fluid Mechanics*, **221**, 1990, pp. 641-673.

2. Lai, Y.G. and So, R.M.C., "Near-wall modelling of turbulent heat fluxes," *International Journal of Heat and Mass Transfer*, **33**, 1990, pp. 1429-1440.

3. So, R.M.C., Zhang, H.S. and Speziale, C.G., "Near-wall modelling of the dissipation-rate equation," *AIAA Journal*, submitted for publication, 1990.

4. Sarkar, L, Erlebacker, G., Hussaini, M.Y. and Kreiss, H.O., "The analysis and modeling of dilatational terms in compressible turbulence," NASA CR-181959, 1989.

5. Hanjalic, K. and Launder, B.E., "A Reynolds-stress model of turbulence and its application to their shear flows," *Journal of Fluid Mechanics*, **52**, 1972, pp. 609-638.

6. Jones, W.P., "Models for turbulent flows with variable density and combustion," **Prediction Method for Turbulent** Flows, (Edited by W. Kollenann), pp. 379-422, Hemisphere, London, 1980.

7. Mansour, N.N., Kim, J. and Moin, P., "Reynolds-stress and dissipation-rate budgets in a turbuelnt channel flow," *Journal of Fluid Mechanics*, **194**, 1988, pp. 15-44.

8. Mansour, N.N., Kim, J. and Moin, P., "Near-wall k-ε turbulence modeling," *AIAA Journal*, **27**, 1989,, pp. 1068-1073.

9. Spalart, P.R., "Direct simulation of a turbulent boundary layer up to $R_\theta = 1410$, " *Journal of Fluid Mechanics*, **187**, 1988, pp. 61-98.

10. Krishnamoorthy, L.V. and Antonia, R.A., "Temperature dissipation measurements in a turbulent boundary layer," *Jouranl of Fluid Mechanics*, **176**, 1987, pp. 265-281.

11. Krishnamoorthy, L.V. and Antonia, R.A., "Turbulent kinetic energy budget in the near-wall region," *AIAA Journal*, **26**, 1987, pp. 300-302.

12. Launder, B.E., "Heat and mass transport," *Turbulence - Topics in Applied Physics*, **12**, edited by P. Bradshaw, Springer, Berlin, 1976, pp. 232-287.

13. Launder, B.E., "On the computation of convective heat transfer in complex turbulent flows," *Journal of Heat Transfer*, **110**, 1988, pp. 1112-1128.

14. Jones, W.P. and Musonge, P., "Closure of the Reynolds-stress and scalar flux equations," *Physics of Fluids*, **31**, 1988, pp. 3589-3604.

15. Newman, G.R.,, Launder, B.E. and Lumley, J.L., "Modelling of the behavior of homogeneous scalar turbulence," *Journal of Fluid Mechanics*, **111**, 1981, pp. 217-232.

16. Elghobashi, S.E. and Launder, B.E., :"Turbulent time scales and the dissipation ratio of temperature variance in the thermal mixing layer," *Physics of Fluids*, **26**, 1983, pp. 2415-2419.

17. Nagano, Y. and Kim, C., "A two-equation model for heat transport in wall turbulent shear flows," *Journal of Heat Transfer*, **110**, 1988, pp, 583-589.

18. Yoshizawa, A., "Statistical modelling of passive-scalar diffusion in turbulent shear flows," *Journal of Fluid Mechanics*, **195**, 1988, pp. 541-555.

19. Shima, N., "A Reynolds-stress model for near-wall and low-Reynolds-number regions," *Journal of Fluids Engineering*, **110**, 1988, pp. 38-44.

20. Coles, D., "Measurements of Turbulent Friction on a Smooth Flat Plate in Supersonic Flow," *Journal of Aeronautical Sciences*, **21**, 1954, pp. 433-448.

21. Wilcox, D. C., "A Complete Model of Turbulence Revisited," AIAA Paper 84-0176, 1984.

22. Anderson, E. C. and Lewis, C. H., "Laminar and Turbulent Boundary-Layer Flows of Perfect Gases or Reacting Gas Mixtures in Chemical Equilibrium," NASA CR-1893, 1971.

23. Morkovin, M., "Effects of Compressibility on Turbulent Flows," Mecanique de la Turbulence, C.N.R.S., edited by A. Favre, 1962, pp. 367-380.

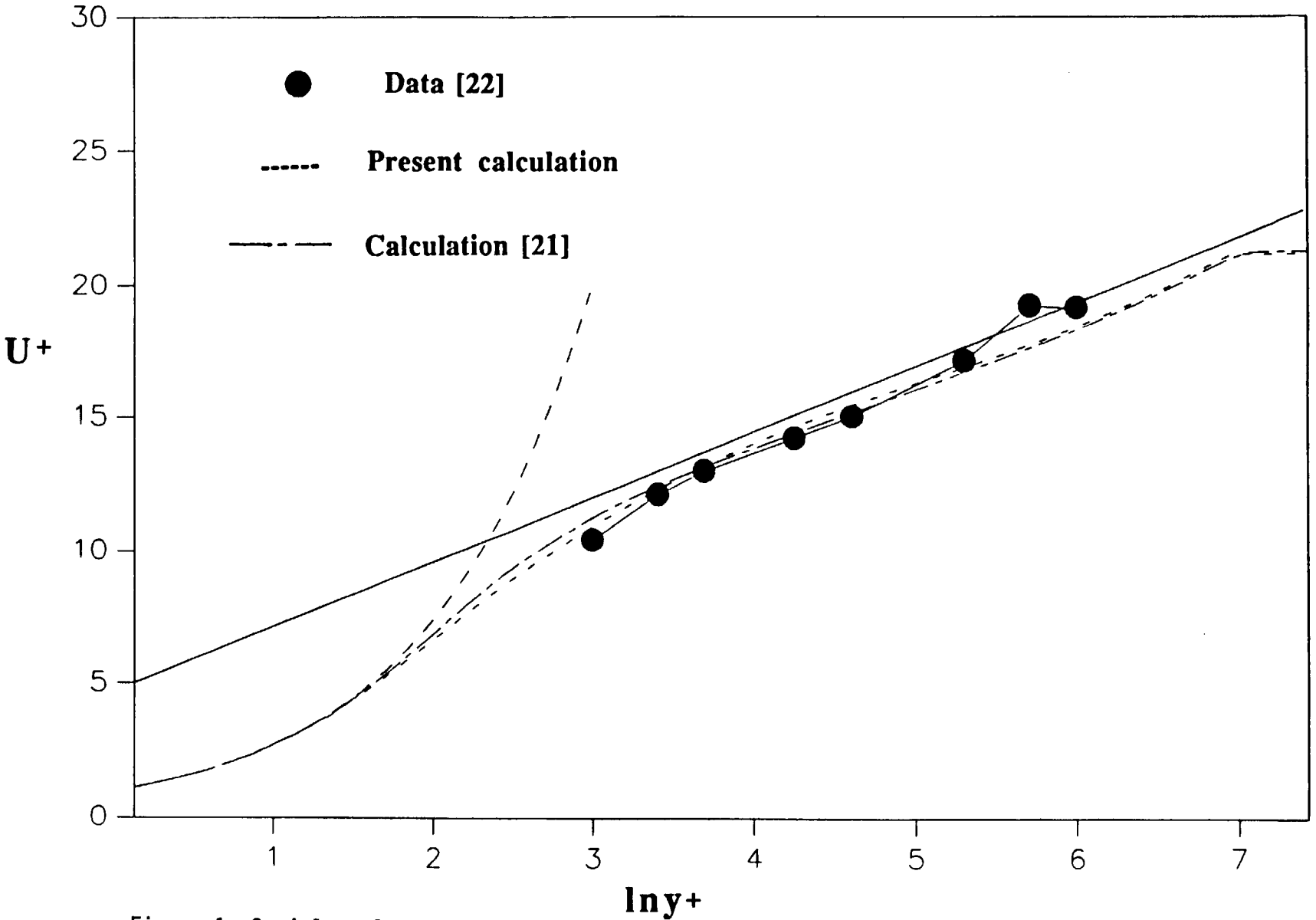

Figure 1. Semi-log plot of mean velocity.

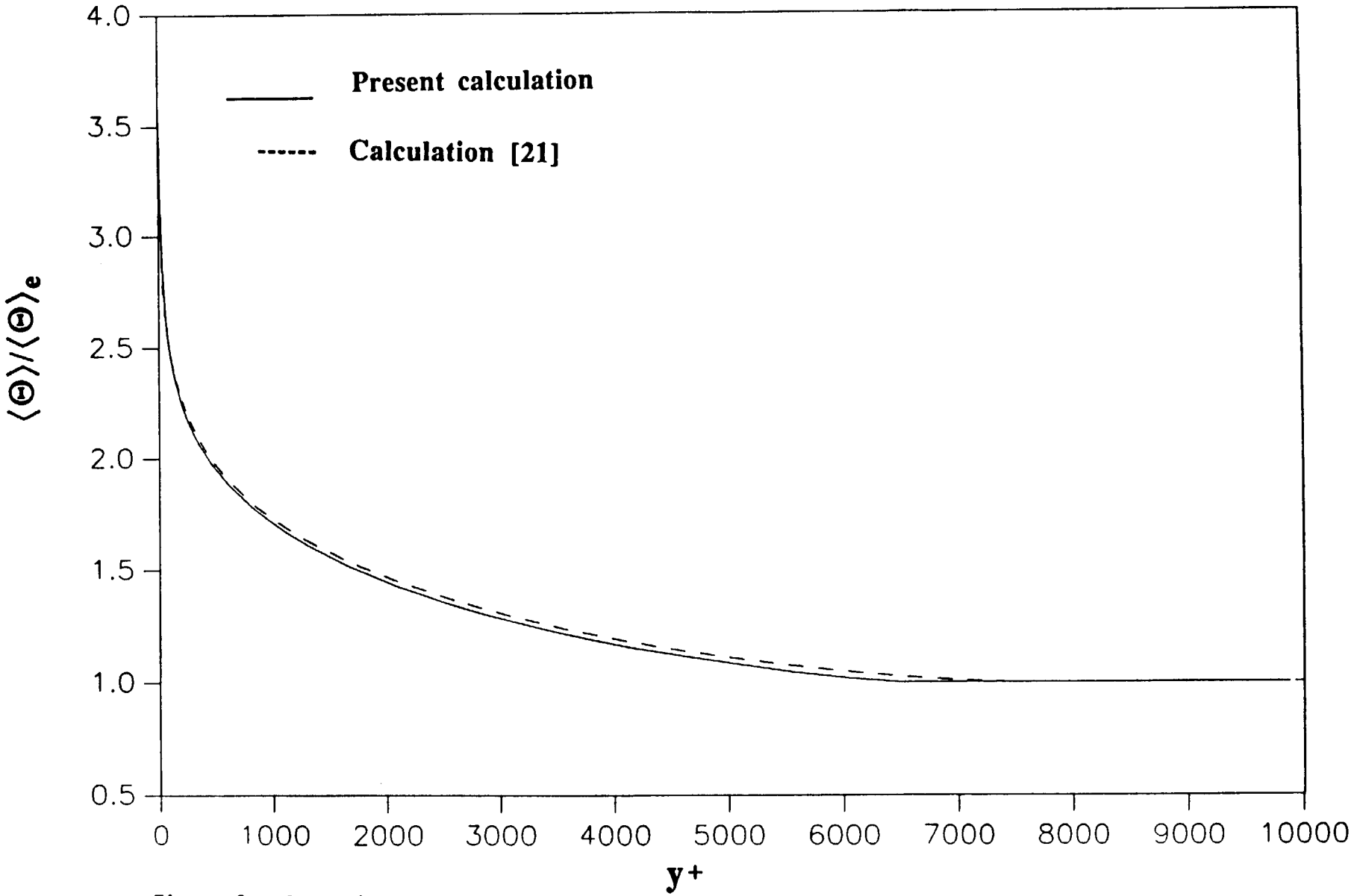

Figure 2. Comparison of calculated mean temperature.

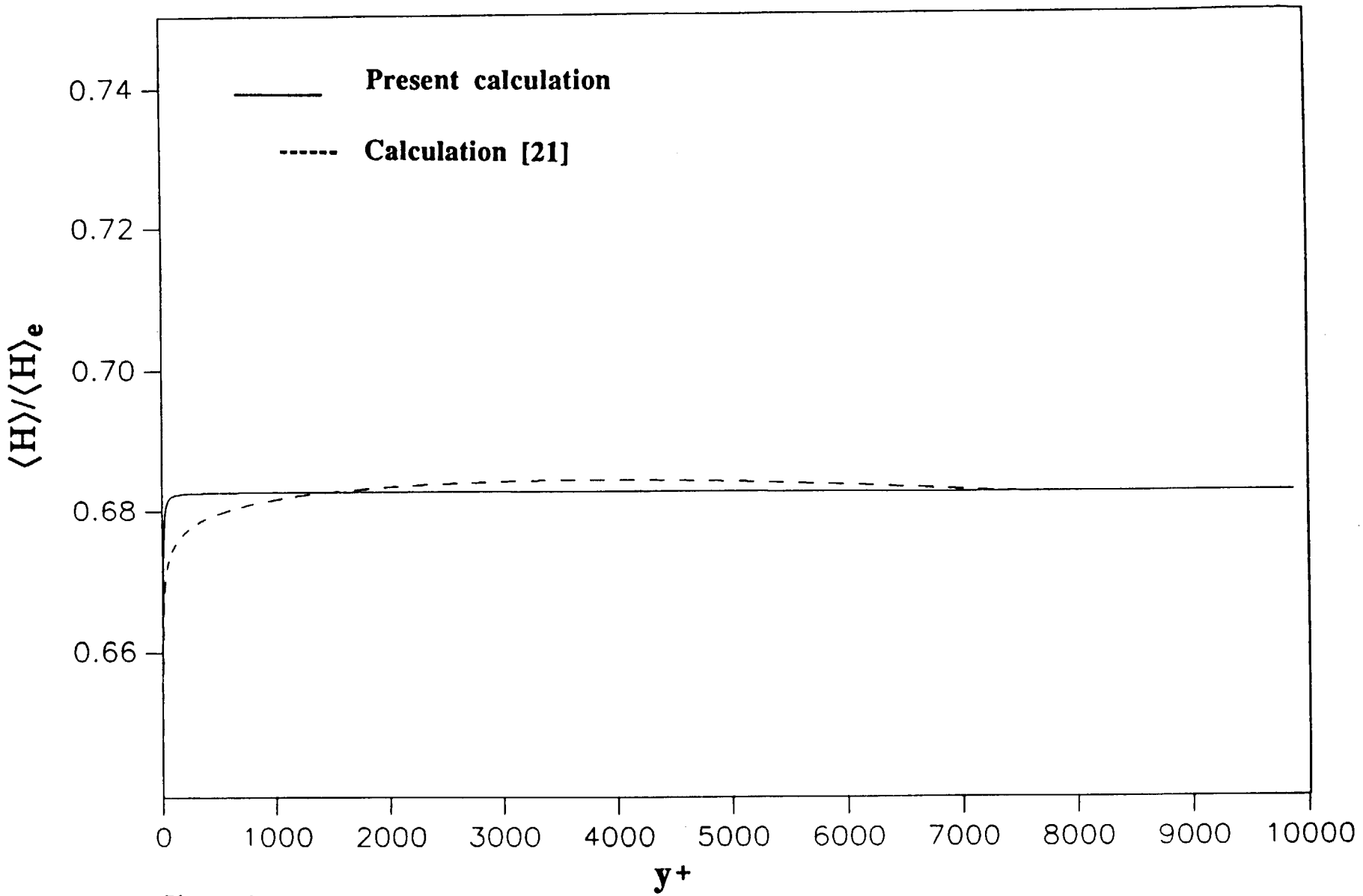

Figure 3. Comparison of calculated mean total enthalpy.

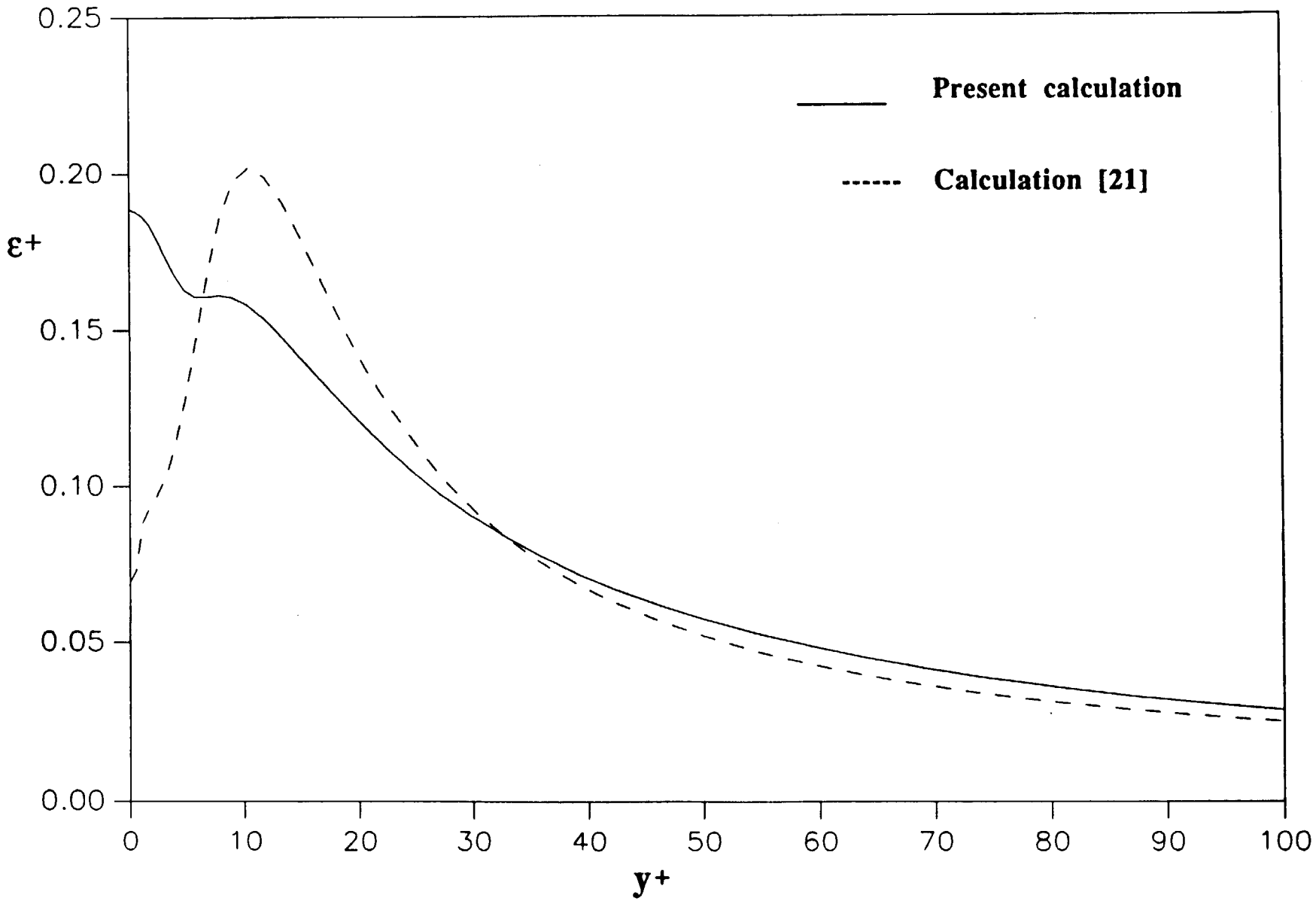

Figure 4. Near-wall behavior of the dissipation function.

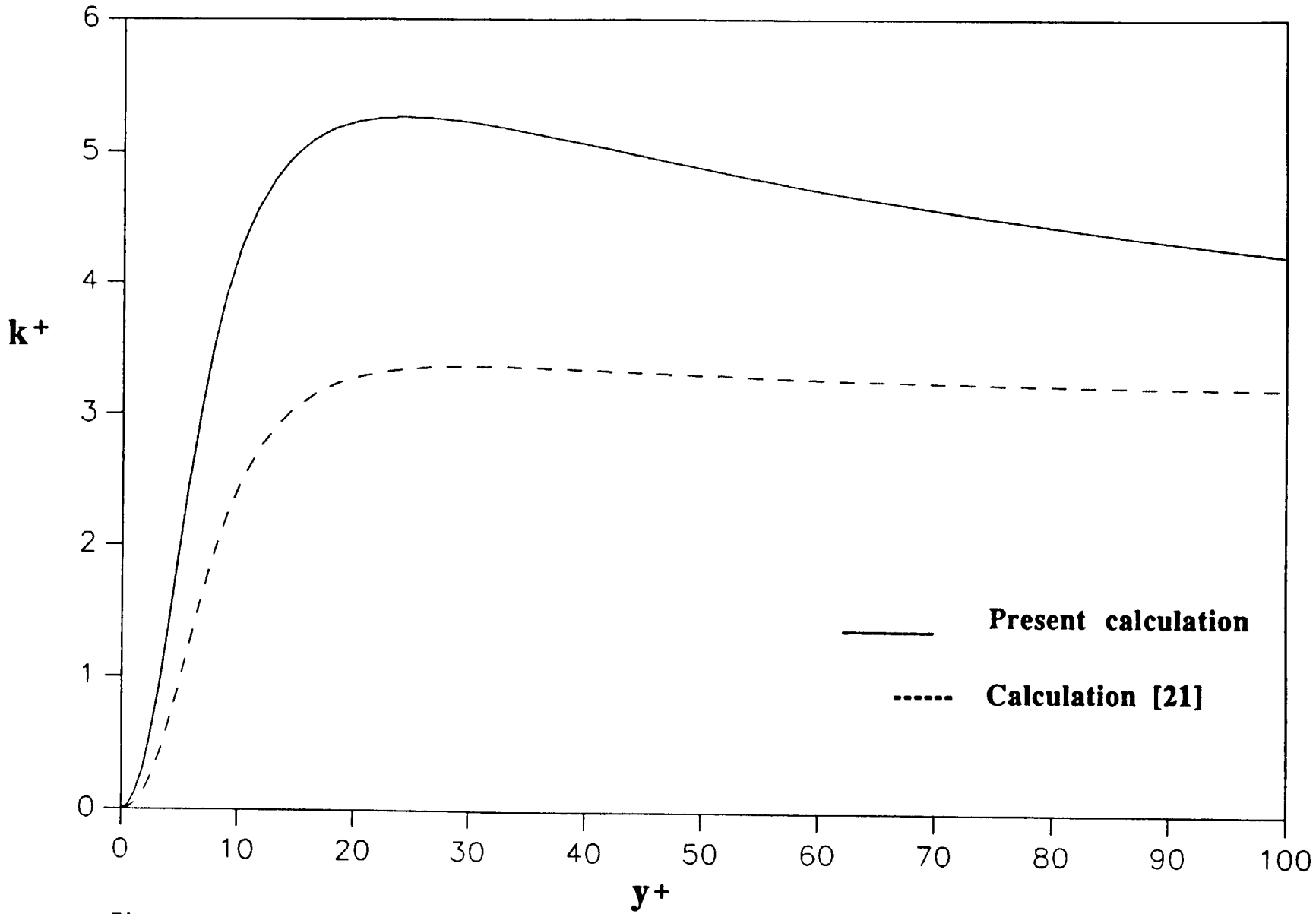

Figure 5. Near-wall behavior of the turbulent kinetic energy.

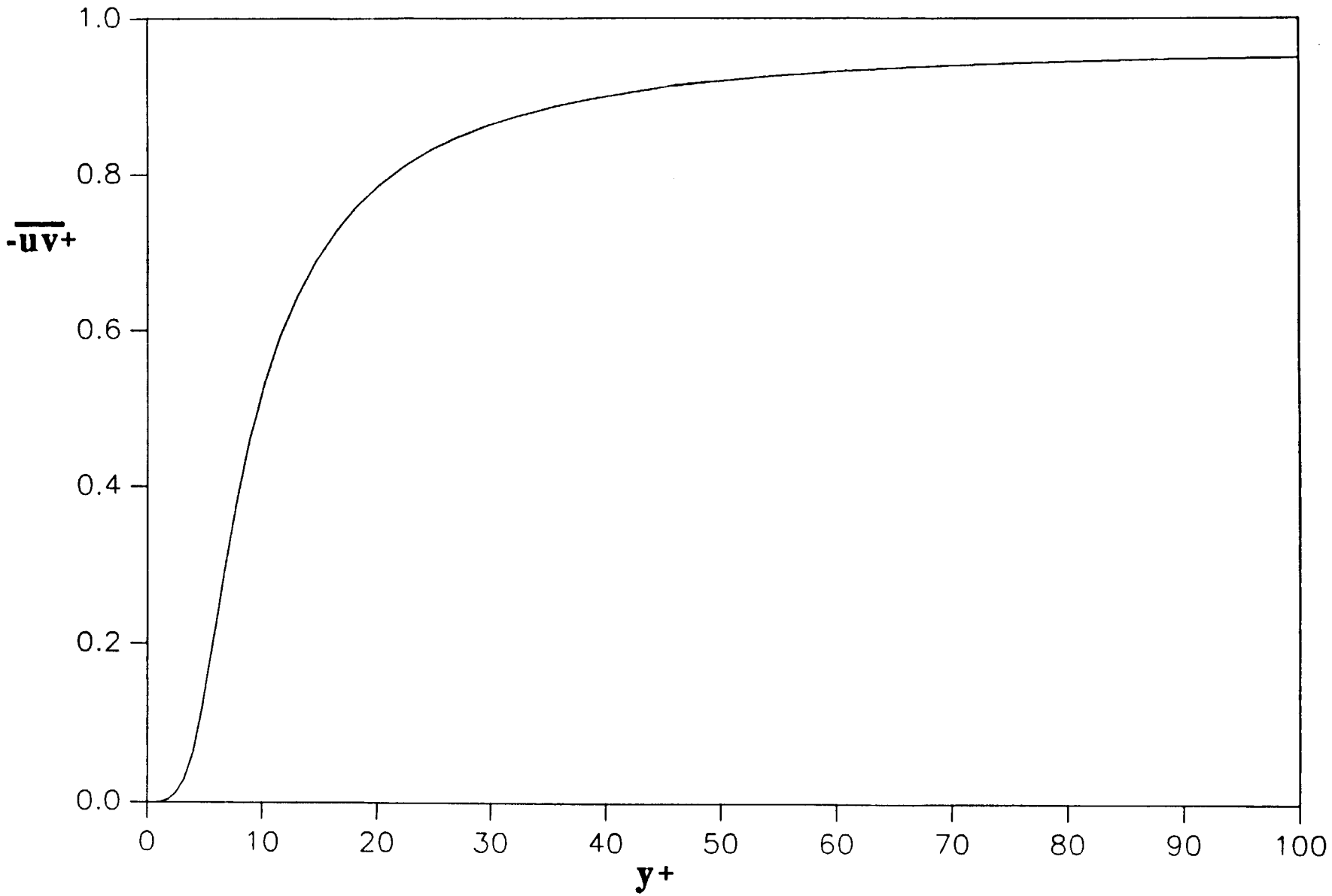

Figure 6. Near-wall behavior of the turbulent shear stress.

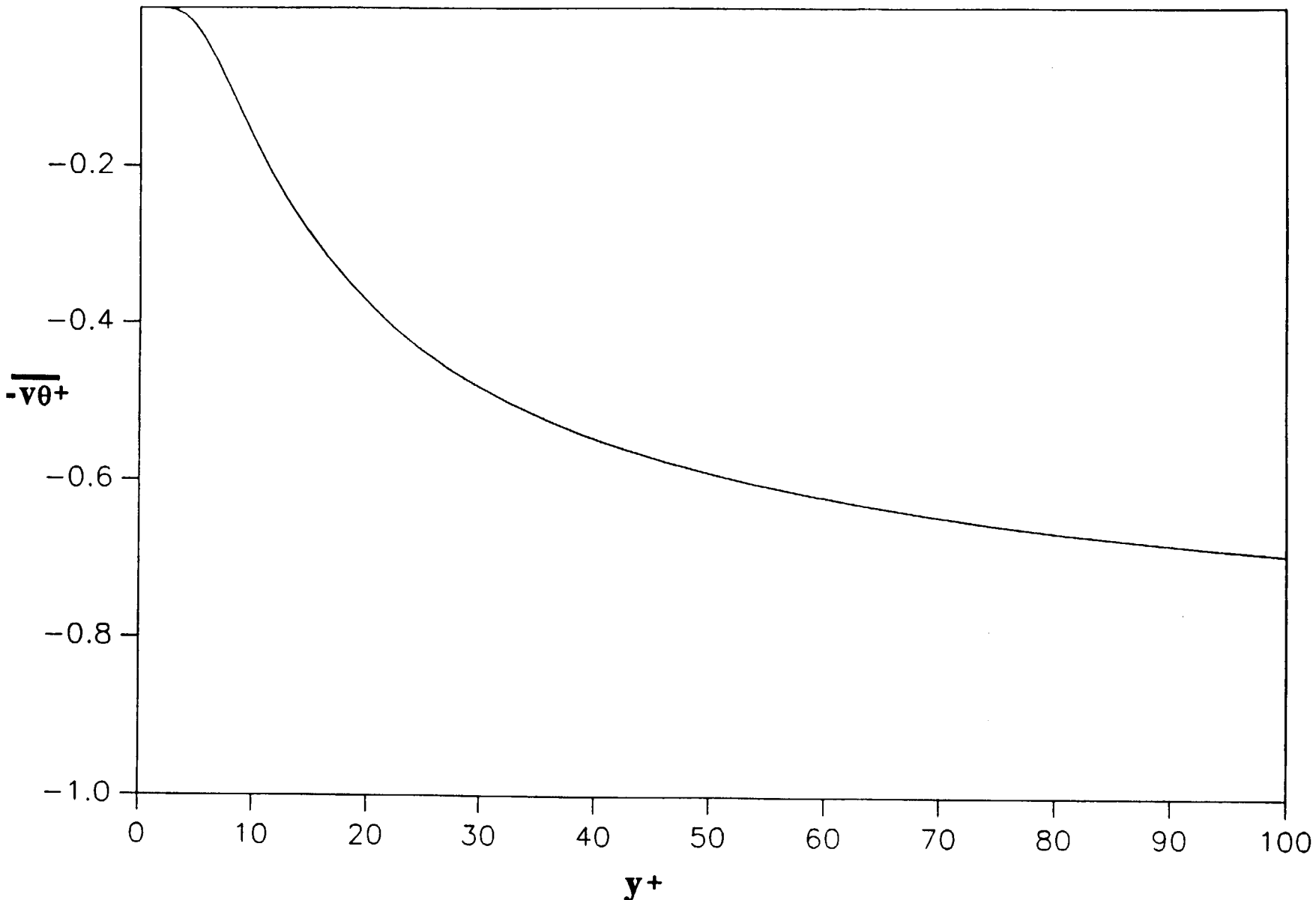

Figure 7. Near-wall behavior of the turbulent heat flux.

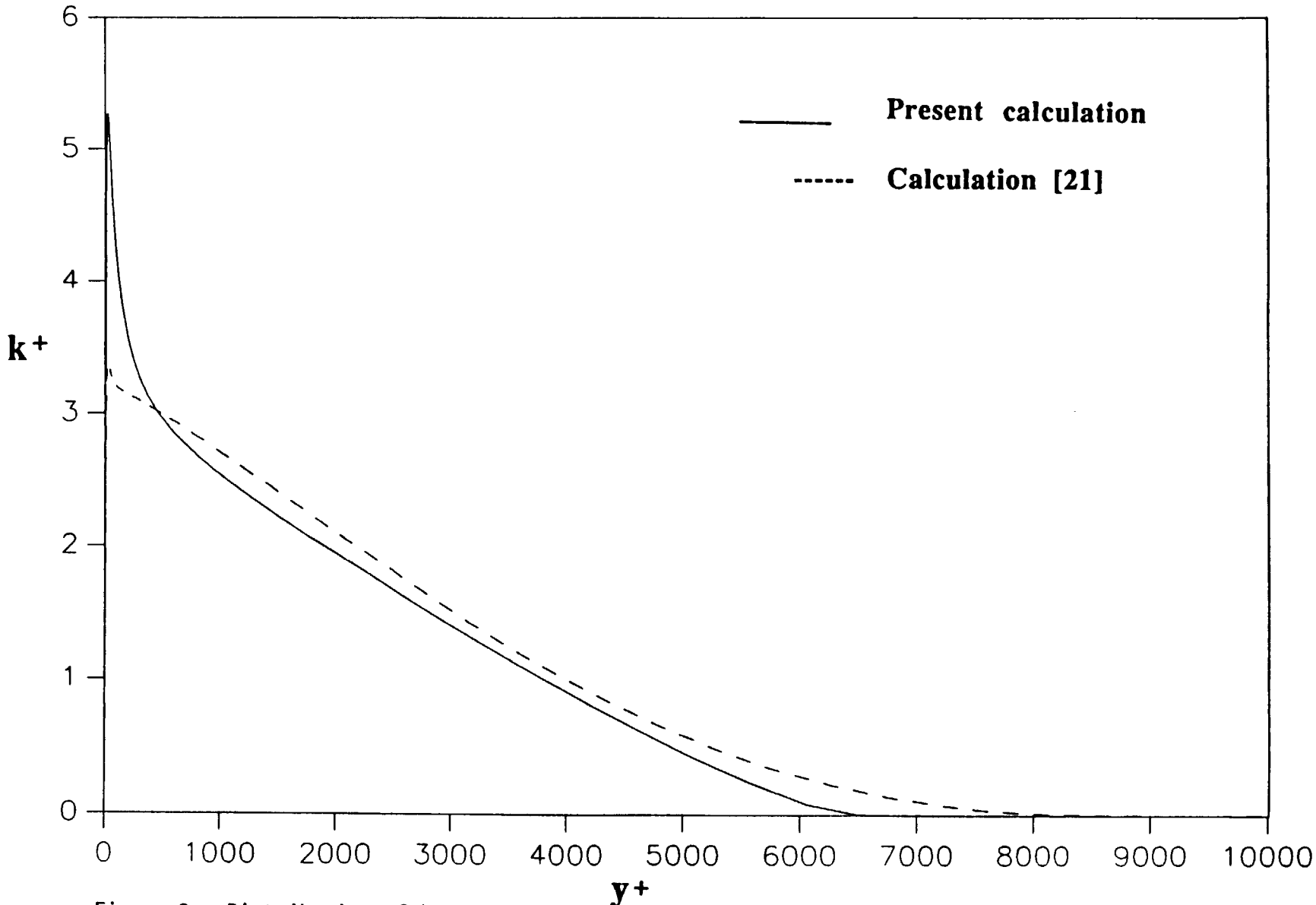

Figure 8. Distribution of k across the boundary layer.

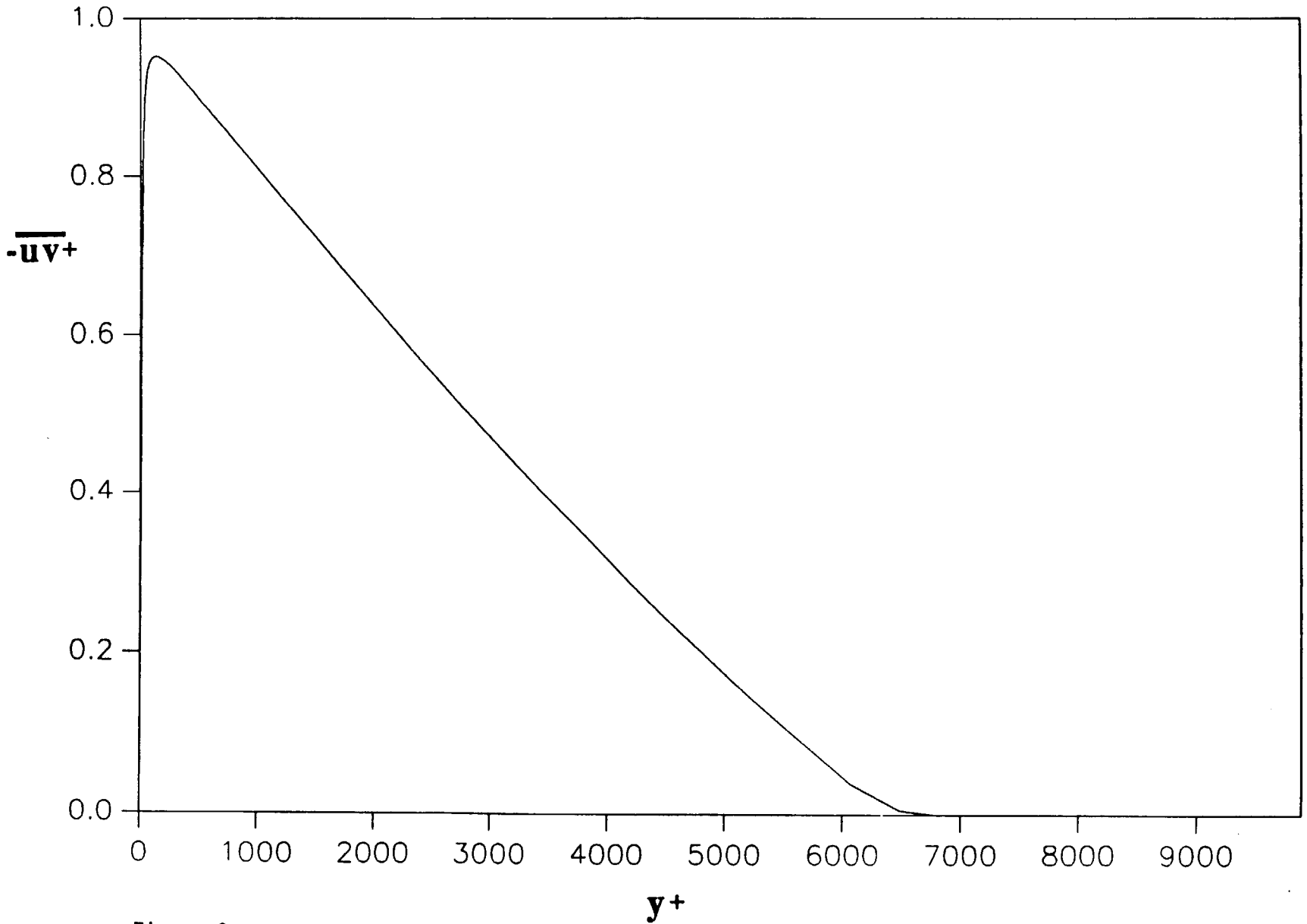

Figure 9. Turbulent shear stress distribution across the boundary layer.

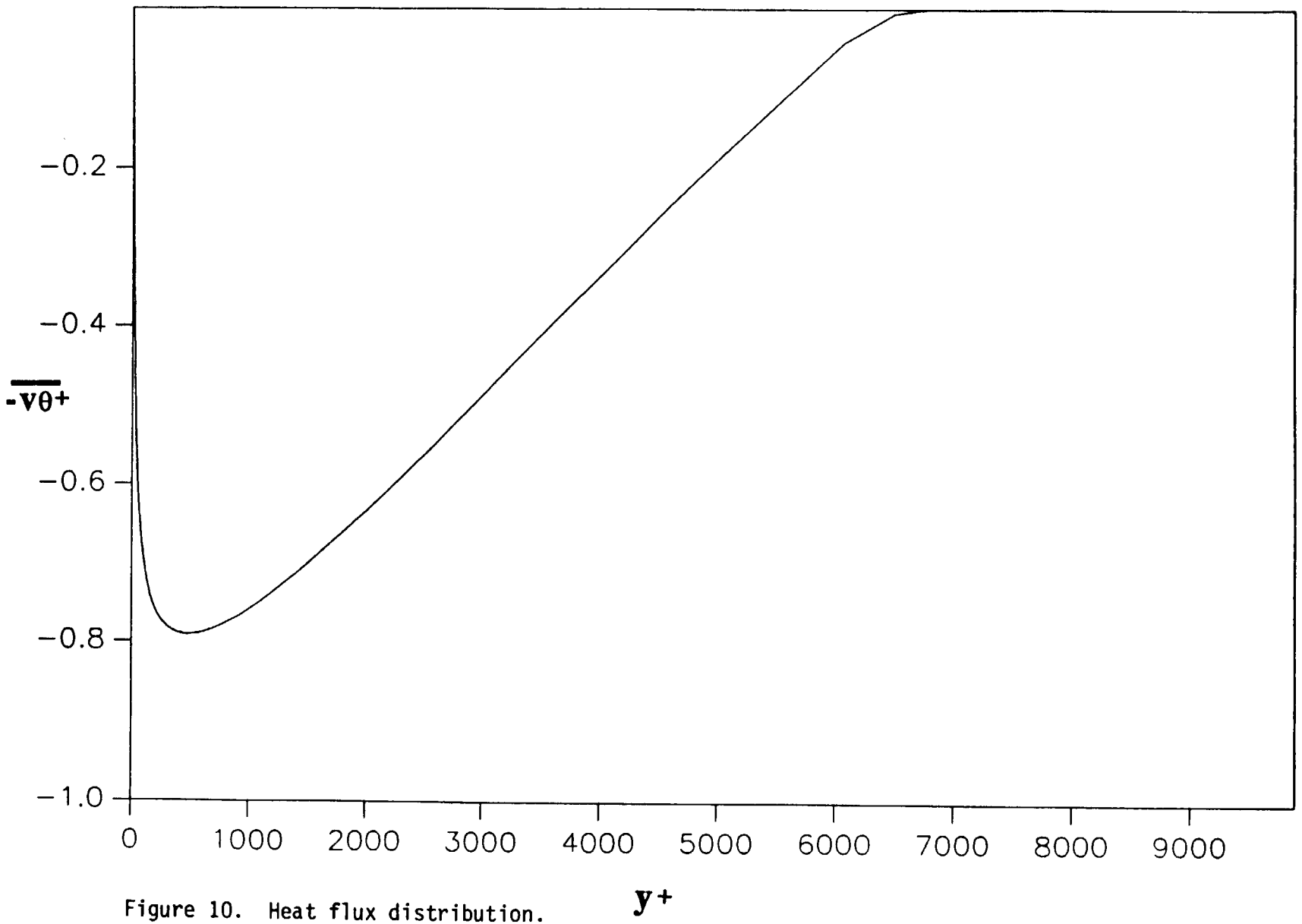

Figure 10. Heat flux distribution.

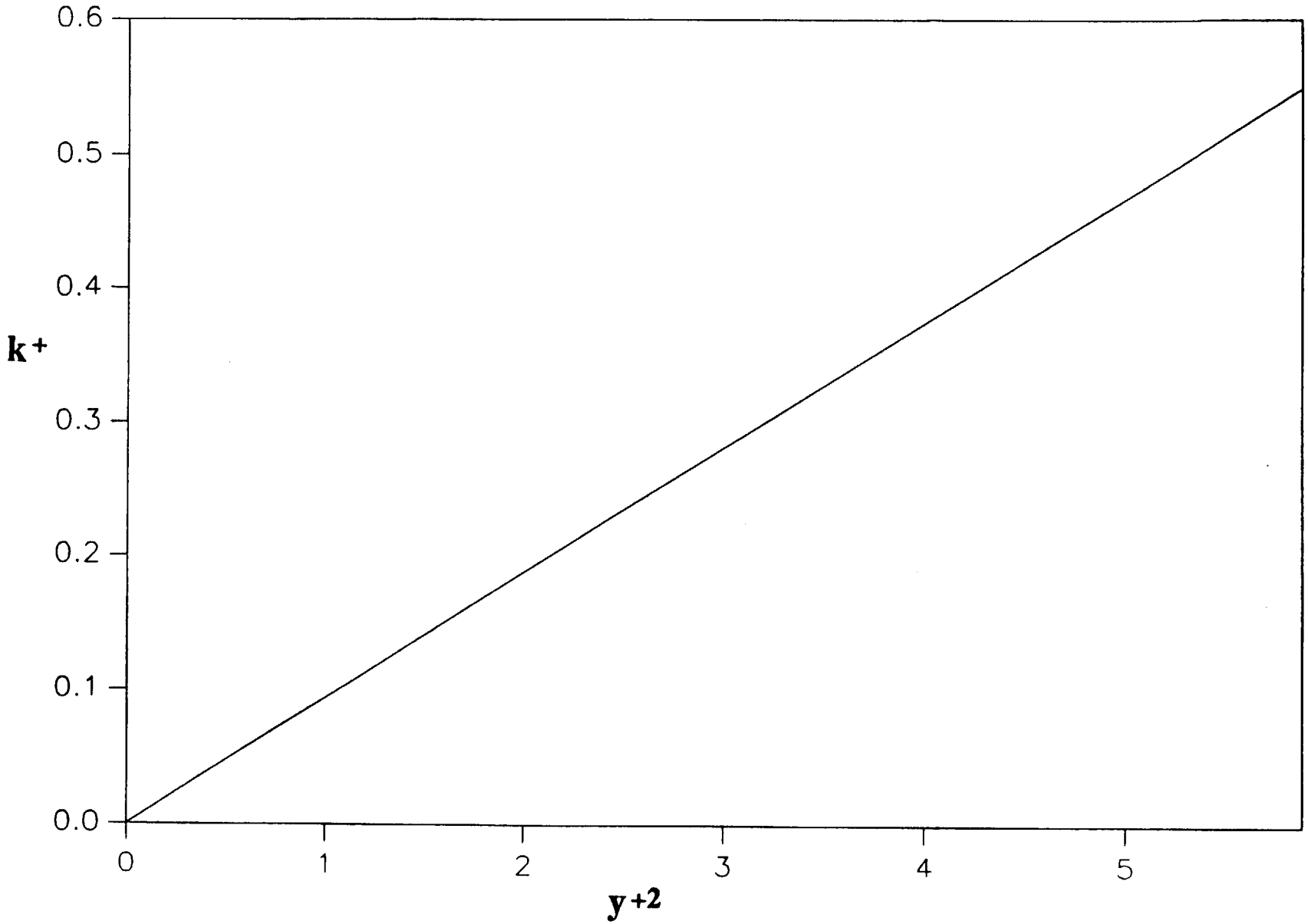

Figure 11. Asymptotic behavior of k at the wall.

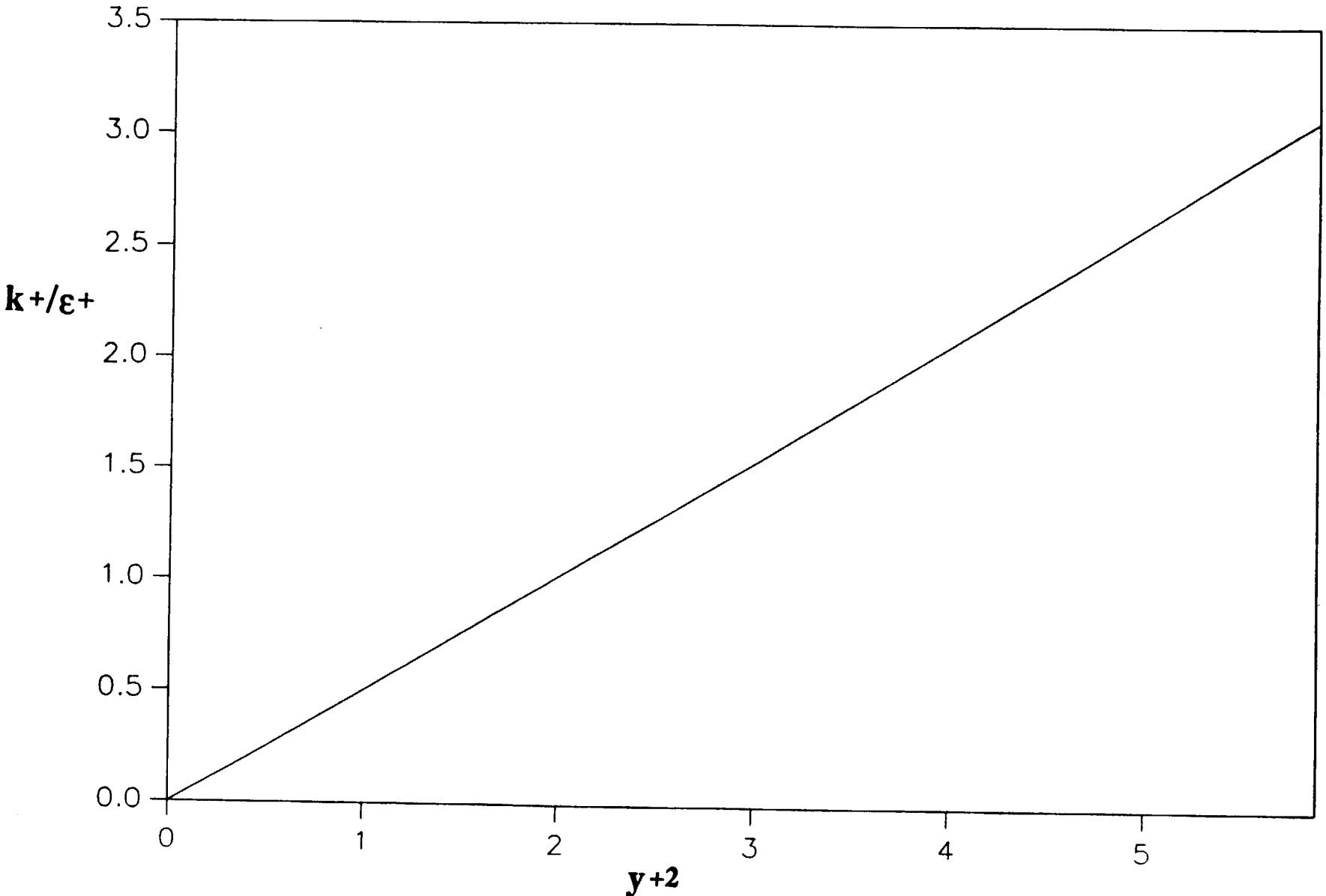

Figure 12. Asymptotic behavior of k and dissipation at tbe wall.

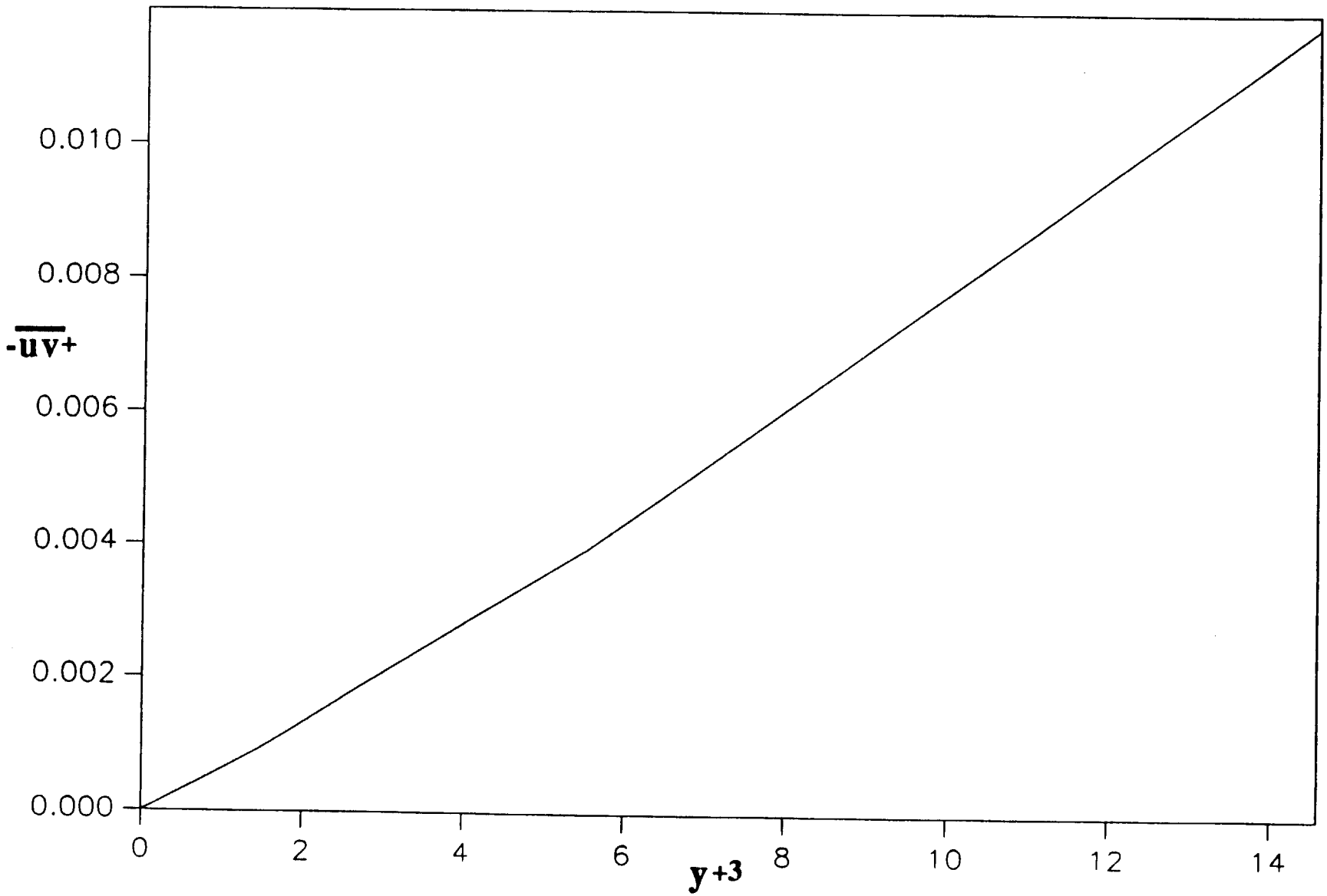

Figure 13. Asymptotic behavior of turbulent shear stress at the wall.

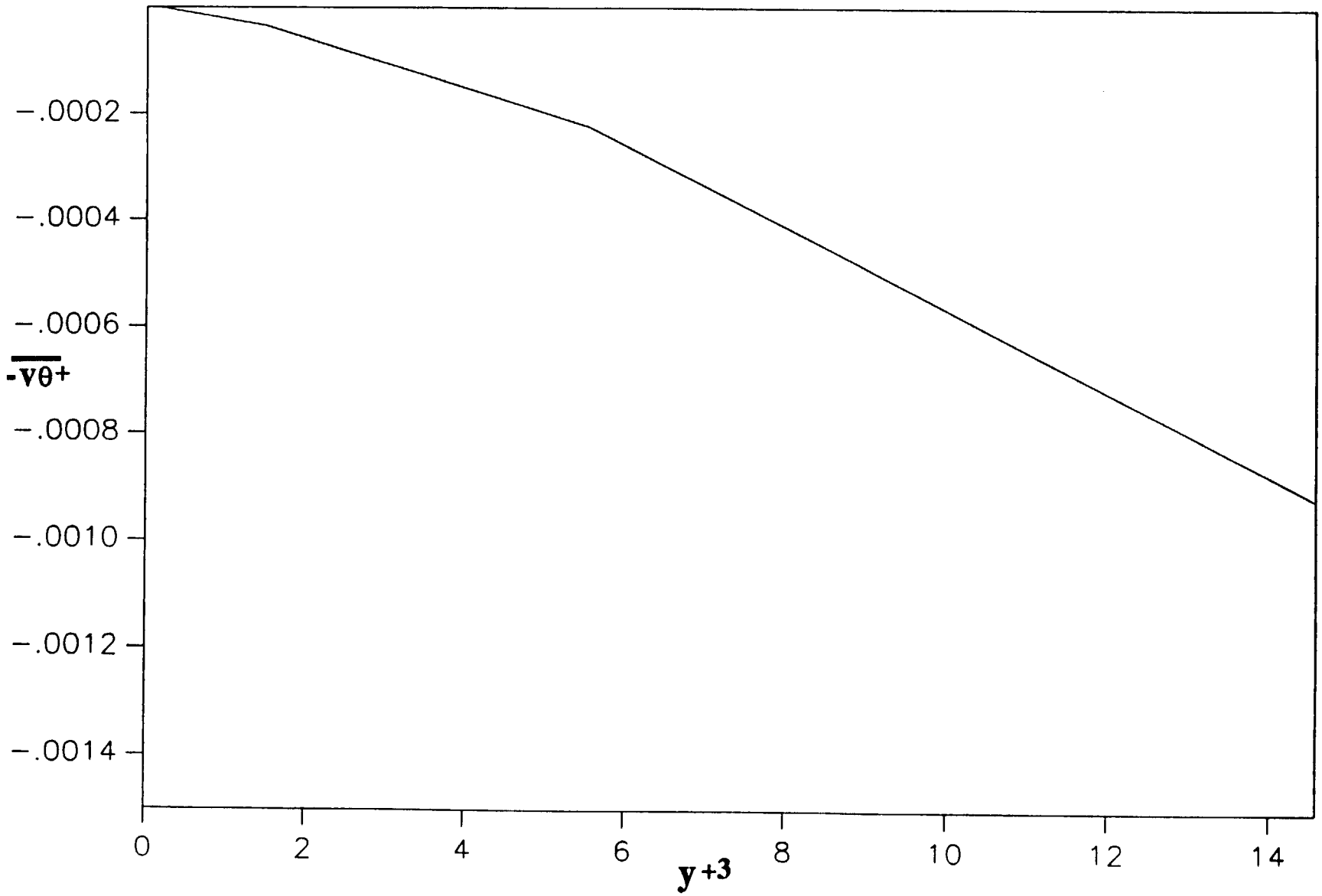

Figure 14. Asymptotic behavior of turbulent heat flux at the wall.